UNIVERSITATEA "POLITEHNICA" DIN BUCUREȘTI
ȘCOALA DOCTORALĂ INGINERIE CHIMICĂ ȘI BIOTEHNOLOGII

TEZĂ DE DOCTORAT
PhD THESIS

METODE MODERNE DE DETECŢIE A CANCERULUI GASTRIC

MODERN METHODS FOR DETECTION OF GASTRIC CANCER

Autor/Author: Doctorand Iuliana Mihaela Bogea
Conducător de doctorat/Scientific Coordinator:
Prof. Dr. habil Raluca-Ioana van Staden

BUCUREȘTI
2022

UNIVERSITATEA "POLITEHNICA" DIN BUCUREȘTI
ȘCOALA DOCTORALĂ INGINERIE CHIMICĂ ȘI BIOTEHNOLOGII

TEZĂ DE DOCTORAT
PhD THESIS

METODE MODERNE DE DETECŢIE A CANCERULUI GASTRIC

MODERN METHODS FOR DETECTION OF GASTRIC CANCER

Autor/Author: Doctorand Iuliana Mihaela Bogea
Conducător de doctorat/Scientific Coordinator:
Prof. Dr. habil Raluca-Ioana van Staden

BUCUREȘTI

Table of Contents

Acknowledgments

I would like to express my thanks and deep gratitude to the PhD coordinator Prof. Dr. habil. Raluca-Ioana van Staden for her outstanding coordination, recommendations and useful advice during my doctoral studies as well as during the elaboration of my PhD thesis.

I would like to express my sincere thanks to the members of the supervisory committee: Prof. Dr. Ing. Ana Maria Josceanu, Prof. Dr. Ing. Gabriel Lucian Radu, Prof. Dr. Cristina Nechifor, who supported and guided me during the PhD school reports.

I would like to thank the team of researchers from the "National Institute for Research and Development of Isotope and Molecular Technologies", Cluj-Napoca, for the synthesis of graphene-based materials and Mr. Marius Bădulescu from the "National Institute for Laser, Plasma and Radiation Physics", Low Temperature Plasma Laboratory, for the synthesis of silver- and carbon-based nanofilms and their characterization by means of SEM and AFM apparatus.

I extend warm thanks to my colleagues in the Electrochemistry and PATLAB Laboratory, especially Ruxandra-Maria Mihai and Damaris-Cristina Gheorghe for their patience, help, and support, as well as for the beautiful collaboration.

I add my thanks for the financial support provided through UEFISCDI, project PN-III-P4-ID-PCCF-2016.

Abstract

Gastric cancer is a silent type of cancer that needs reliable tools and screening tests for its early detection in order to increase the rate of survival. Therefore, in this PhD thesis there were developed stochastic and voltametric sensors as screening tools for gastric cancer. Covering wide ranges of linear concentrations with very low detection limits being the only sensors that can make a reliable qualitative analysis of the sample, stochastic sensors were used for the molecular recognition and quantification of p53, maspin as well as enantioanalysis of aspartic acid and arginine in different biological samples: whole blood, tumoral tissues, urine, and saliva. The screening methods were validated and are in use in clinical studies in order to be standardized and approved for the early detection of gastric cancer.

Introduction

Gastric cancer is a silent type of cancer. Usually, it is detected in advanced stages, when the chances of survival are very low. Gastric cancer, ranks fourth in the world, being among the most common types of cancer and the second most common cause of death worldwide, especially in Asian countries such as China.

Therefore, developing screening tests for the early detection of gastric cancer is a need. Different therapies for gastric cancer were developed [1-7]; chemotherapeutic agents were developed for stopping the rapid multiplication and spread of cancer cells. An effective method in the rapid and correct detection of gastric cancer is represented by the analysis of specific biomarkers, which indicate the stage of gastric cancer.

The most used types of biomarkers are: nucleic acids, carbohydrates, proteins, lipids, small metabolites, cytogenetic and cytokinetic parameters and tumor cells in biological fluids that control physiological and pharmacological processes [8]. A significant role in tumor metastasis is played by carcinoembryonic antigen and may be partially associated with the detection of gastric cancer. Studies on serum markers for gastric cancer have found an increase in CEA levels in patients with gastric cancer [11]. Another biomarker is the p53 protein, a tetrameric phosphoprotein that mediates signal transduction from damaged DNA to genes involved in cell cycle organization and apoptosis. In human cancer, the p53 tumor suppressor gene undergoes different types of mutations that cause the accumulation of nonfunctional proteins [12]. In healthy patients, the p53 protein is present in small amounts in biological fluids. Accumulated proteins can be detected in tissues, blood and other fluids in the human body [15]. Mutations in the p53 gene are significantly correlated with the overexpression of the p53 protein and contribute to genetic predisposition in gastric cancer patients [13 - 14]. Following research over time, it was concluded that a specific tumor marker is expressed only in tumor cells. Most tumor antigens, such as embryonic antigens (alpha fetoprotein and carcinoembryonic antigen) are unique (specific) to the individual tumor, being expressed during embryological development and in cancer cells. Carcinoembryonic antigen (CEA) is expressed in all types of gastrointestinal, pancreatic and breast

cancer [15, 16]. Tumor suppressor protein p53 plays an important role in the growth and evolution of cancer and its response to chemotherapy [17 - 27]. Various studies indicate the association of overexpression of tumor suppressor protein p53 in relation to gastric cancer, resulting in a short time of tumor survival [28 - 30]. Maspin is a relatively new biomarker that can be used in the screening tests for early detection of gastric cancer.

Electrochemical sensors have become a good alternative to the standard methods used in clinical laboratories (e.g., ELISA, chemiluminescence), due to the determination directly from the sample of patients of the compounds of interest and the remarkable selectivity and sensitivity [31], they being successful also in environmental analysis [32], biotechnology [33] and process control [34, 35].

While CEA, p53, maspin are also indicating the presence or other diseases in the body, scientists have come to the conclusion that enantioanalysis of the amino acids may give a better indication for the presence of gastric cancer. Studies have shown that tryptophan is the metabolite with the most repeated changes in several types of risky diseases. Esophageal cancer patients decreased plasma measurements of 14 separate amino acids, including tyrosine, phenylalanine, and tryptophan [36,37].

This thesis addresses modern electrochemical methods of analysis, based on stochastic and voltammetric sensors as screening tools for early detection of gastric cancer. Stochastic sensors have many advantages over conventional electrochemical sensors, are sensitive and selective, having the ability to simultaneously determine several compounds of interest in very small amounts of analyzed sample, covering wide ranges of linear concentrations with very low detection limits and are the only sensors that can make a reliable qualitative analysis of the sample. Molecular recognition and quantification of p53, maspin as well as enantioanalysis of aspartic acid and arginine were performed in different biological samples. The screening methods were validated and are in use in clinical studies in order to be standardized and approved for early detection of gastric cancer.

Chapter 1: Stochastic Sensors

1.1 Introduction

Stochastic sensors are devices used in a very wide range to determine different analytes. They are needed in many fields, having a wide applicability in different fields; for example, in the environment they are used to determine various pollutants, minerals, and other chemical forms that can affect air quality and thus quality of life; they can also be used in the German industry to determine various compounds. Also, in case of war, stochastic sensors are used to determine the toxic gases used as chemical weapons, the explosives used in the case of terrorist attacks or the presence of unexploited mines [38, 43]. In medicine, sensors have experienced a favorable evolution, being used as screening tools for various pathologies, by determining various biomarkers specific for certain diseases. They are very useful in determining the levels of therapeutic agents that need to be monitored, for example: microorganisms, toxins present in the body's fluid [38].

1.2 Mechanism of the Response of the Stochastic Sensors

The method used by stochastic sensors is based on channel conductivity. In the stochastic method the optimal working potential is chosen in order to achieved the best sensitivity for the measurements. The determination of the biomarkers takes place in two steps [38, 39]:

1) molecular recognition stage: the analyte of interest it is extracted from the solution at the membrane-solution interface, enters the channel, and blocking it until it is fully placed inside; therefore, the intensity of the current became zero until the full analyte is passing through the hole inside the channel; the period of time needed to get inside the channel is known as the analyte signature (marked as t_{off}). This step is also known as the qualitative analysis step of the biomarkers/analytes;
2) binding and electroanalysis stage: This stage takes place when the analyte interacts with the channel wall and redox processes take place. The analyte binding equation is:

$$Ch(i) + Analyte(i) \leftrightarrow Ch \bullet Analyte(i);$$

where Ch=pore channel, i= the interface at which the reaction takes place.

The time required for this stage is known as the quantitative parameter, denoted by t_{on}. This parameter is used to determine the concentration of the analyte/biomarkers in the samples. The step is also known as quantitative analysis step.

1.3 Design of the Stochastic Sensors

The design of stochastic sensors (Fig. 1) is very important in the analysis of samples, it is simple, cheap, using in most cases carbon-based matrices. To prepare the stochastic sensor, choose a powder (based on graphite, graphene, diamond, etc.) to which a certain amount of paraffin oil is added to ensure a perfect homogenization. To this paste is added the material capable of forming channels / pores (based on e.g., porphyrins, cyclodextrins, ionic liquids, etc.) that allow stochastic analysis. The paste thus formed is inserted into a plastic tube inside which a silver wire is inserted to ensure electrical contact. Before each use, the stochastic sensor is washed well with deionized water so as not to contaminate the other samples used for analysis, after which it is dried with great care, thus being prepared for a new measurement of a new sample [38,43].

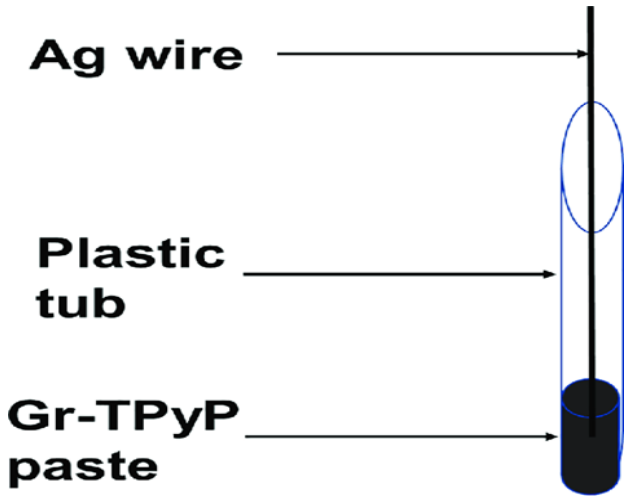

Fig.1. Design of stochastic sensors

1.4 Sensitivity and Selectivity of the Stochastic Sensors

The sensitivity recorded in the stochastic mode is far higher than those recorded for other electrochemical sensors. The sensitivity is given by the slope of the calibration graph of the stochastic sensor.

The selectivity of the stochastic sensors is connected with the first stage of the mechanism of the response of the stochastic sensors - the molecular recognition stage. The selectivity is given by the signature of the analyte(s) and interfering species (t_{off} parameter) which has a unique value depending on the size, geometry, length, capacity of unfolding, and speed of the analyte(s) and interferent species. The difference in signatures is giving the selectivity. Stochastic sensors proved to have high selectivity, and therefore they can be used for simultaneous assay of more than 10 biomarkers in biological fluids.

1.5 Applications of the Stochastic Sensors in Biomedical Analysis

Stochastic sensors have been intensively applied in the medical field, both as a method of diagnosis, screening and to determine the developmental stages of various pathologies. They have been used to analyze biomarkers for diabetes, for various types of cancer, for obesity, for early puberty, for inflammatory diseases, etc. The screening methods based on stochastic sensors compared to commercial tests such as ELISA, RIA, etc. have multiple advantages: short analysis time, very low detection and determination limits (which allow analysis for extremely low concentrations, requiring a small amount of sample to be analyzed), high selectivity (sensors being selective for each analyte in part), a low cost. Stochastic sensors allow a limited applicability (determination of a single analyte of interest) or very wide, of a panel of biomarkers (simultaneous determination of several analytes) being used both for whole blood samples and for air, saliva, urine and other fluids. of the body (e.g., cerebrospinal fluid). For diabetes, stochastic sensors were used to determine glucose, IL-1β, IL-6, IL-12, IL-17; leptin, PAI-1 (plasminogen activator inhibitor1), CRP, adiponectin, zinc, etc.

Chapter 2: Biomarkers Used in the Diagnosis of Gastric Cancer

2.1 Introduction

Biomarkers are formed immediately when the tumor is forming in the body. Analysis of biomarkers can be done for diagnostic of cancer as well as for establishing the efficiency of the treatments [44-49]. Early-stage diagnostic is rare especially in gastric cancer [50-52]. An effective method in the rapid and correct detection of cancer is represented by the analysis of specific biomarkers, which may also indicate the stage of gastric cancer. The most used types of biomarkers are: nucleic acids, carbohydrates, proteins, lipids, small metabolites, cytogenetic and cytokinetic parameters and tumor cells in biological fluids that control physiological and pharmacological processes [53].

Chapter 3: Enantioanalysis of Aspartic Acid Using 3D Stochastic Sensors

3.3 Results and Discussions

3.3.1 Response Characteristics of the 3D Stochastic Sensors

The response characteristics of the proposed 3D stochastic sensors were shown in Table 3.1. Different signatures (t_{off} values) of the enantiomers determined when the same 3D stochastic sensor was used proved that the enantiomers can be simultaneous recognized and determined in samples, and that the 3D-stochastic sensors were enantioselective. (Table 3.1) For the assay of L-Asp the wider linear concentration range (between $1x10^{-15}$ and $1x10^{-2}$mol L^{-1}) and the highest sensitivity ($1.51x10^{11}s^{-1}$/mol L^{-1}) were recorded for the 3D stochastic sensor based on SEGr-1; the result can be correlated with the content of Sulphur in the graphene – the higher the content, the best sensitivity. Also, for the assay of D-Asp the wider linear concentration range (between $1x10^{-12}$ and $1x10^{-2}$mol L^{-1}) and the highest sensitivity ($5.46x10^{8}s^{-1}$/mol L^{-1}) were recorded for the 3D

stochastic sensor based on SEGr-1. Accordingly, the 3D stochastic sensor of choice is the one based on SEGr-1.

Table 3.1. Response characteristics of the 3D stochastic sensors used for the enantioanalysis of aspartic acid.

3D stochastic sensors based on	Calibration equation* and correlation coefficient (r)	Linear concentration range (mol L^{-1})	t_{off} (s)	Sensitivity (s^{-1}/mol L^{-1})	Limit of quantification (mol L^{-1})
L-Asp					
PIX/SEGr-1	$1/t_{on}=0.04+1.51x10^{11}xC$ r=0.9993	10^{-15}-10^{-2}	1.3	$1.51x10^{11}$	10^{-15}
PIX/SEGr-2	$1/t_{on}=0.02+3.91x10^{7}xC$ r=0.9985	10^{-11}-10^{-2}	1.3	$3.91x10^{7}$	10^{-11}
D-Asp					
PIX/SEGr-1	$1/t_{on}=0.04+5.46x10^{8}xC$ r=0.9998	10^{-12}-10^{-3}	1.7	$5.46x10^{8}$	10^{-12}
PIX/SEGr-2	$1/t_{on}=0.02+3.30x10^{7}XC$ r=0.9989	10^{-11}-10^{-3}	1.7	$3.30x10^{7}$	10^{-11}

*$<1/t_{on}>$ = s^{-1}, <C> = mol L^{-1}

3.3.2 Selectivity of the 3D Stochastic Sensors

The selectivity of the stochastic sensors is given by the signature of the different biomarkers/analytes obtained using the same sensors. Different signatures (t_{off} values) of the supposed interference analytes indicated selectivity. First, the enantioselectivity was verified by the signatures of the enantiomers of L-and D-Asp (Table 3.1); for each of the 3D stochastic sensor the signatures of the enantiomers were different, proving the enantioselectivity of the sensors. Other amino acids such as leucine, tryptophan, glutamine were checked as possible interferences. All of them had different signatures than L- and D-Asp proving that the proposed 3D stochastic sensors are selective.

3.3.3 Stability of the 3D Stochastic Sensors

The proposed sensors were tested for a period of 6 month when their sensitives varied with 0.85% for the 3D stochastic sensor based on SEGr-1, and 0.95% for the 3D stochastic sensor based on SEGr-2. These results proved a very good stability of the proposed 3D stochastic sensors.

3.4 Enantioanalysis of Aspartic Acid in Whole Blood Samples

The 3D stochastic sensors were used as tools for the screening tests of whole blood samples. The whole blood was placed into the electrochemical cell, and the signatures of L- and D-Asp were determined in the diagrams obtained (Figure 3.1). Based on the measurements of t_{on} values for each enantiomer identified (based on its signature, Table 3.1) in the diagram, the concentration was determined using the stochastic method described above.

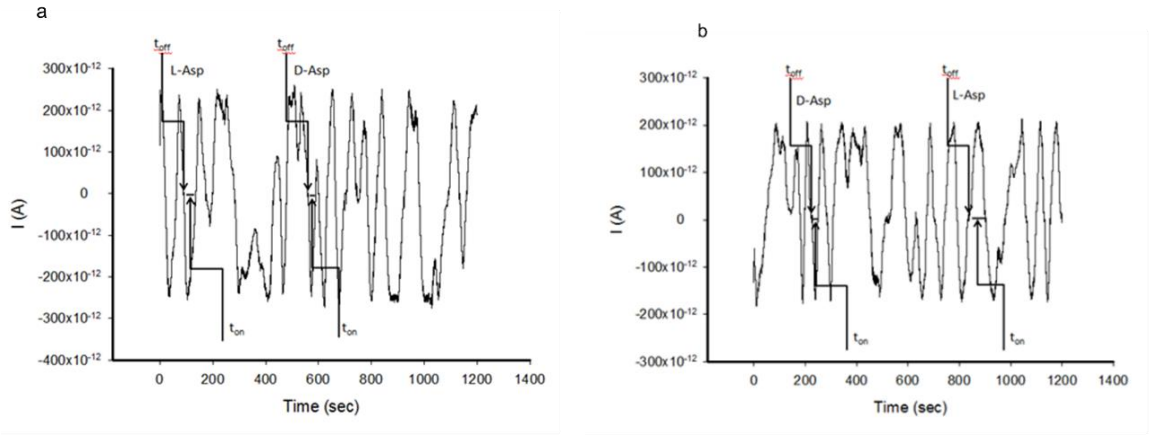

Figure 3.1 Diagrams recorded for the enantioanalysis of Asp in whole blood samples using the 3D stochastic sensors based on: (a) PIX/SEGr-1, and b) PIX/SEGr-2.

First, for the validation of the 3D stochastic sensors and of the screening method, whole blood samples from healthy patients were spiked with L- and D-Asp. Only L-Asp was found in these samples – before the addition of well-known amounts of L- and D-Asp, in different ratios. After the addition of the enantiomers, the quantities of L- and D-Asp were determined accordingly with the stochastic method; the results obtained in Table 3.1 shown high recoveries in whole blood samples of L- in the presence of D-Asp, and of D-Asp in the presence of L-Asp.

Table 3. 1. Recovery tests of one enantiomer in the presence of the other enantiomer (N=10).

3D stochastic sensors based on	**Enantiomer**	**Recovery (%)**			
	D:L	**2:1**	**1:1**	**1:2**	**1:10**
PIX/SEGr-1	L-Asp	99.21 ±0.08	99.95±0.07	99.90±0.07	99.15±0.05
PIX/SEGr-2	L-Asp	98.23 ±0.12	98.75±0.10	98.87±0.08	99.07±0.07
	L:D	**2:1**	**1:1**	**1:2**	**1:10**
PIX/SEGr-1	D-Asp	99.12±0.05	99.65±0.05	99.97±0.08	99.12±0.08
PIX/SEGr-2	D-Asp	99.15±0.03	98.98±0.04	98.12±0.07	98.90±0.07

Whole blood samples collected from healthy people, as well as whole blood samples collected from patients confirmed with gastric cancer were used for the validation of the screening test. Table 3.2 shows the results obtained for the whole blood collected from healthy donors; only the L-Asp was found in the whole blood samples collected from the healthy people. Table 4 shows the results of the screening test for the whole blood collected from patients with gastric cancer; both L- and D-Asp were found in the whole blood of patients confirmed with gastric cancer. Paired t-tests were also used for the validation of the 3D stochastic sensors used as tools in the screening tests of whole blood. The paired t-tests were performed at 99.00% confidence level. All calculated values for the pair-t test at the 99.00% confidence level were less than the tabulated theoretical value: 4.032 (Tables 3.2, and 3.3).

Table 3.2. Enantioanalysis of Asp in whole blood samples of patients confirmed with gastric cancer.

Sample no.	Enantiomer of aspartic acid*	3D Stochastic sensor based on	
		PIX/SEGr-1	PIX/SEGr-2
1	L	16.57±0.03	16.59±0.08
	D	19.55±0.03	18.90±0.08
2	L	70.05±0.04	70.11±0.07
	D	11.70±0.05	11.69±0.07
3	L	42.23±0.05	43.54±0.07
	D	24.91±0.03	24.80±0.06
4	L	14.43±0.02	15.67±0.07
	D	17.73±0.02	17.41±0.08
5	L	16.63±0.05	16.02±0.08
	D	17.88±0.04	16.35±0.08
6	L	25.39±0.05	26.99±0.06
	D	24.91±0.04	24.22±0.05
7	L	69.38±0.03	68.89±0.05
	D	42.60±0.05	40.40±0.08
8	L	11.33±0.05	11.50±0.08
	D	28.36±0.03	26.13±0.08
9	L	14.43±0.02	15.62±0.09
	D	22.43±0.02	22.09±0.09
10	L	19.49±0.04	18.85±0.07
	D	17.73±0.03	17.12±0.07
t-test			2.76

*All results are expressed in μmol L^{-1} (N=10).

Table 3.3. Enantioanalysis of Asp in whole blood samples of healthy patients.

Sample no.	Enantiomer of aspartic acid*	3D Stochastic sensor based on	
		PIX/SEGr-1	PIX/SEGr-2
1	L	641.18±0.02	641.24±0.06
2	L	194.86±0.02	199.26±0.07
3	L	469.53±0.03	472.73±0.07
4	L	178.98±0.04	179.60±0.08
5	L	194.85±0.05	197.16±0.05
6	L	403.76±0.02	408.80±0.07
7	L	118.98±0.02	131.40±0.07
8	L	880.75±0.03	879.64±0.06
9	L	118.98±0.04	119.90±0.07
10	L	855.02±0.02	854.05±0.07
t-test			2.25

*All results are expressed in μmol L^{-1} (N=10).

Accordingly, there is no statistically significant difference between the results obtained for the screening tests using the 3D stochastic sensors, at 99.00% confidence level., for the enantioanalysis of Asp in whole blood samples. Accordingly, the screening method and the 3D stochastic sensors can be validated for the enantioanalysis of Asp in whole blood samples. The advantages of using such method compared with those proposed earlier [140,141] are: the design of the sensors is fast and easy to be made in a very short time (no special equipment is needed); the reliability (sensitivity, selectivity, recovery tests) is higher; qualitative and quantitative assay of the enantiomers of aspartic acid can be reliable performed.

Chapter 4: N, S Decorated Graphene Modified with 2,3,7,8,12,13,17,18-octaethyl-21H,23H-porphine Manganese (III) Chloride Based 3D Needle Stochastic Sensors for Enantioanalysis of Arginine – a Key Factor in the Metabolomics and Early Detection of Gastric Cancer

4.2.6 Design of the 3D Enantioselective Needle Stochastic Sensors

The graphene pastes were prepared by mixing paraffin oil with each of the N, S co-doped graphene powder (NS-Gr-1 and NS-Gr-2) (Figure 4.2). The modifier, porphyrin complex (0.001 mol L^{-1} prepared in THF), was added to the graphene paste in a ratio of 1:1 (v:w, mL:mg). Plastic non-conducting tubes with the inner diameter of 3.00 mm were filled with the modified paste. A silver wire was used as the contact between the paste and the external circuit (Figure 4.3). Before and after each measurement, the microsensors were cleaned with deionized water and, when not in use, the sensors were stored at room temperature.

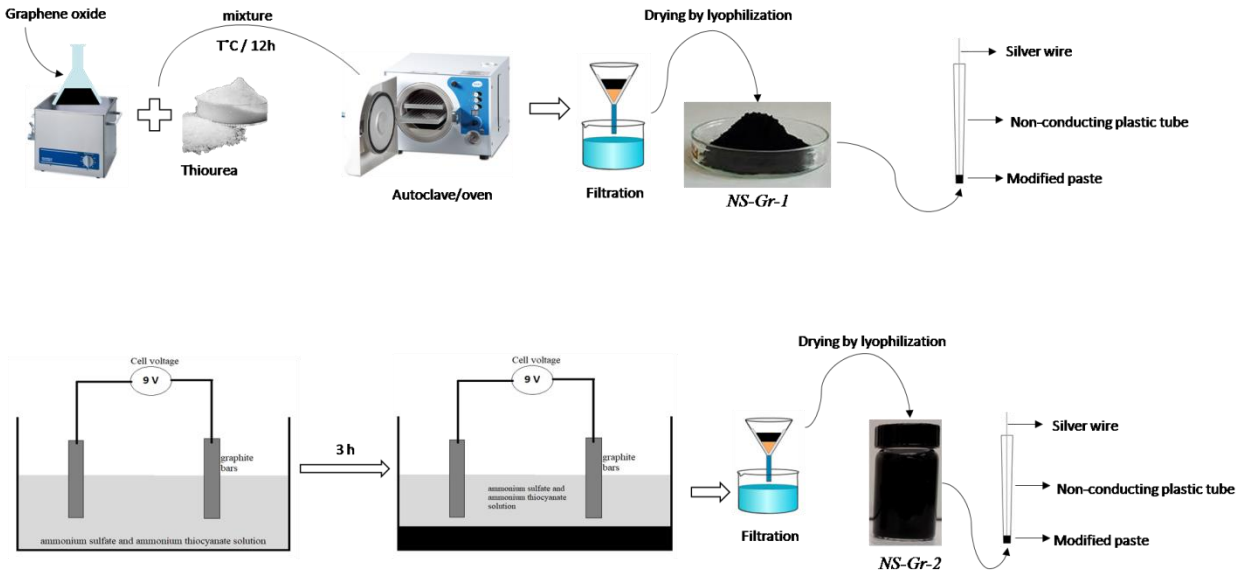

Figure 4.2. The preparation of the graphene powders and the design of the stochastic sensors.

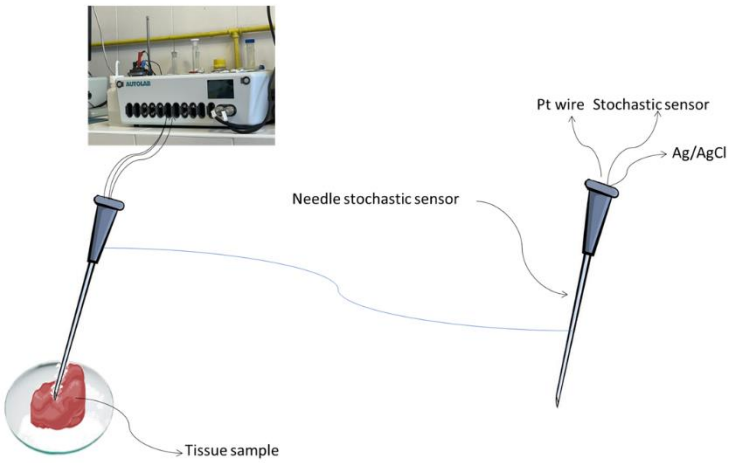

Figure 4.3. The experimental set-up of used in the enantioanalysis of arginine.

4.2.7 Stochastic Mode

The chronoamperometric method was used for the qualitative and quantitative analysis of L- and D-arginine based on their signature (t_{off} value). The quantification of the analytes was done using the t_{on} values (Figures 4.4–4.5 and Table 4.2). A constant potential of 125 mV was applied for the determination of L- and D-arginine. The designed 3D enantioselective needle stochastic

sensors were introduced into a cell containing solutions of analyte of different concentrations. Calibration relationships were obtained for both 3D enantioselective needle stochastic sensors. The calibration equations were determined using the linear regression method.

Table 4.2. Response characteristics of the 3D enantioselective needle stochastic sensors used for the enantioanalysis of arginine.

3D Enantioselective needle stochastic sensors based on MnPorph and NS co-doped graphene	**Calibration equation* and correlation coefficient (r)**	**Linear concentration range (mol L^{-1})**	**t_{off} (s)**	**Sensitivity (s^{-1}/mol L^{-1})**	**Limit of quantification (mol L^{-1})**	**Limit of detection (mol L^{-1})**
L-arginine						
NS-Gr-1	$1/t_{on}=0.02+2.27x10^{11}xC$ r=0.9999	$1.0x10^{-15}$ – $1.0x10^{-2}$	2.2	$2.27x10^{11}$	$1.0x10^{-15}$	$2.5x10^{-16}$
NS-Gr-2	$1/t_{on}=0.04+1.54x10^{10}xC$ r=0.9998	$1.0x10^{-14}$ – $1.0x10^{-3}$	1.4	$1.54x10^{10}$	$1.0x10^{-14}$	$2.8x10^{-15}$
D-arginine						
NS-Gr-1	$1/t_{on}=0.01+6.56x10^{11}xC$ r=0.9999	$1.0x10^{-15}$ – $1.0x10^{-3}$	4.4	$6.56x10^{11}$	$1.0x10^{-15}$	$2.1x10^{-16}$
NS-Gr-2	$1/t_{on}=0.01+4.18x10^{10}xC$ r=0.9999	$1.0x10^{-14}$ – $1.0x10^{-2}$	2.4	$4.18x10^{10}$	$1.0x10^{-14}$	$2.2x10^{-15}$

*$<1/t_{on}>$ = s^{-1}; <C> = mol L^{-1}

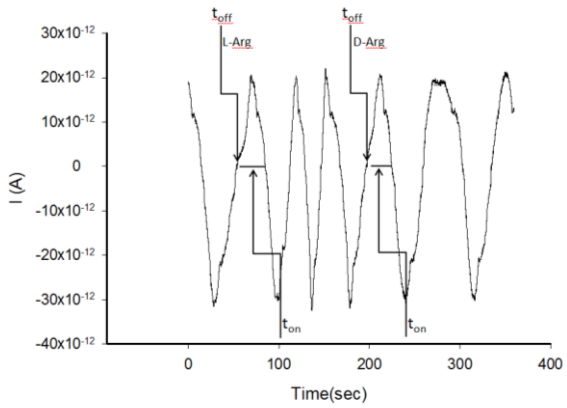

(a)

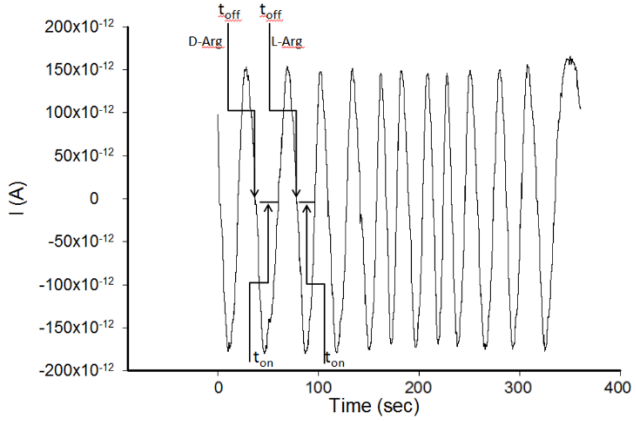

(b)

Figure 4.4. Enantioanalysis of arginine in whole blood samples, using 3D enantioselective needle stochastic sensors based on MnPorph and: (a) NS-Gr-1 b) NS-Gr-2.

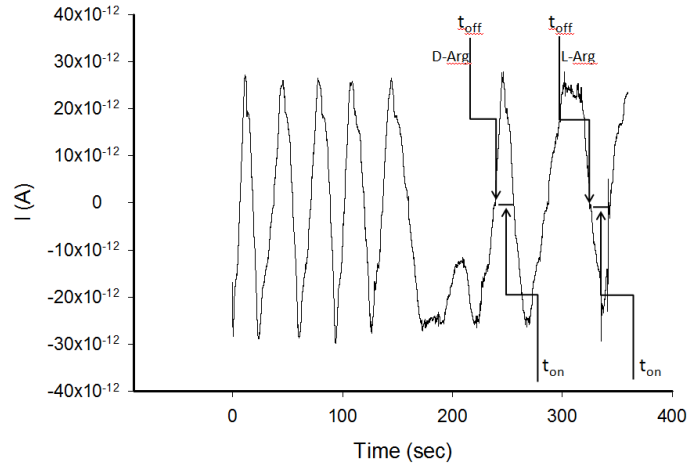

(a)

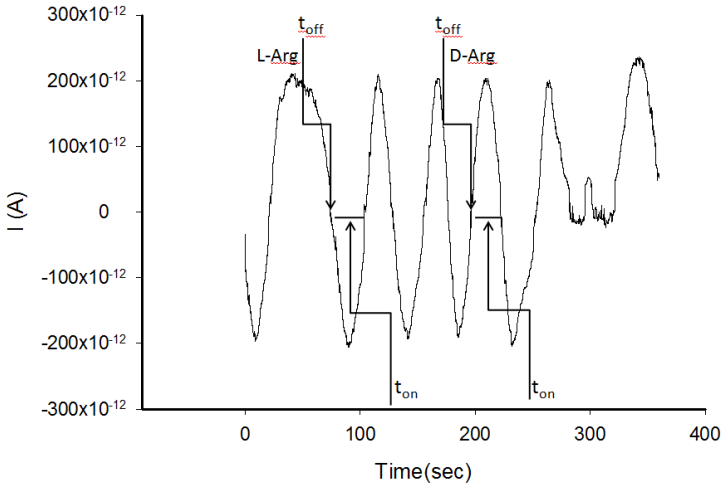

(b)

Figure 4.5. Enantioanalysis of arginine in tissue samples using 3D enantioselective needle stochastic sensors based on MnPorph and: a) NS-Gr-1; b) NS-Gr-2.

Biological samples, such as whole blood and tissue samples (Ethics committee approval nr. 32647/2018 awarded by the County Emergency Hospital from Targu-Mures) from confirmed patients with gastric cancer were used for the screening tests for the enantioanalysis of arginine without any pre-treatment, just after they were taken from patients. Venous blood samples were taken from GC patients and control groups, into tubes containing ethylenediaminetetraacetic acid (EDTA). Tissue samples were analyzed immediately after being collected from the patients; the

sensors were introduced in the tissue (collected during surgery in sterile tubes containing phosphate buffer) for the measurements. Informed consent was obtained from all patients.

4.3 Results and Discussions

4.3.1 Response Characteristics of the 3D Enantioselective Needle Stochastic Sensors

All response characteristics were determined using chronoamperometry at a constant potential of 125 mV vs Ag/AgCl, following the stochastic mode described above. The response characteristics from Table 4.2 show that the proposed sensors are enantioselective; different signatures (t_{off} values) were recorded for the L- and D-enantiomer of arginine, when the same stochastic sensor was used. The linear concentration ranges recorded for both stochastic sensors were very wide, covering levels found in healthy patients (upper levels in the concentration ranges), but also in patients confirmed with gastric cancer (middle to lower levels in the concentration ranges) [155]. The limits of quantification (the lowest concentration from the linear concentration range) are 1 fmol L^{-1} for L-arginine and 10 fmol L^{-1} for D-arginine. Very low limits of detection were also recorded. High sensitivities were recorded for both stochastic sensors when used for the enantioanalysis of arginine; the highest values were recorded when NS-Gr-1 was used as matrix: $2.27x10^{11}$ mol L^{-1} for the assay of L-arginine, and $6.56x10^{11}$ mol L^{-1} for the assay of D-arginine.

4.3.2 Selectivity of the 3D Enantioselective Needle Stochastic Sensors

The selectivity of the proposed stochastic sensors is given by the signatures recorded for the enantiomers of arginine versus the signatures of other compounds in the biological samples; the difference between signatures gives the selectivity. Amino acids such as tryptophan (Try), glutamine (Glu), serine (Ser), and glutathione (GSH) were considered as possible interferences; the recorded signatures, shown in Table 4.3, proved that the proposed stochastic sensors are selective versus these amino acids.

Table 4.3. Selectivity of the 3D enantioselective needle stochastic sensors used for the enantioanalysis of arginine.

3D Enantioselective needle stochastic sensors based on MnPorph and NS co-doped graphene	Signature, t_{off} value						
	L-arg	D-arg	L-glu	D-glu	GSH	Try	Ser
NS-Gr-1	2.2	4.4	0.5	1.0	3.2	1.5	2.7
NS-Gr-2	1.4	2.4	0.7	1.8	3.5	2.8	3.2

4.3.3 Stability and Reproducibility Measurements

Ten 3D enantioselective needle stochastic sensors from each of the two types (10 based on NS-Gr-1 and 10 based on NS-Gr-2) were designed; the values of the sensitivities recorded for the 10 sensors of each type proved that there are no significative changes in the sensitivity, its variation for each type being lower than 0.10 %; this proved the reproducibility of the design of each type of stochastic sensor. After 30 days of measurements, the recorded variation of the sensitivities for the NS-Gr-1 based stochastic sensor was 0.13 %, while for the NS-Gr-2 based stochastic sensor was 0.22 %; this proved that the sensors are stable for at least one month, when daily measurements are performed.

4.4 Enantioanalysis of Arginine in Whole Blood and Gastric Tumor Tissue Samples

Fresh whole blood and gastric tumor tissue samples from patients confirmed with gastric cancer were used as taken from the patients; no sampling was applied to these samples. The stochastic mode measurements described above was used to determine the presence of the enantiomers of arginine in these samples, and also in samples collected from healthy volunteers. The first step in reading the diagrams obtained after the screening of the real samples was to find the signature (t_{off} value) of each enantiomer, followed by the reading (in between two consecutive t_{off} values) of the t_{on} value (Figures 4.4 and 4.5). The results obtained for the screening of the whole blood and gastric tumor tissue samples from patients confirmed with gastric cancer are shown in Table 4.4, while the results obtained after the screening of whole blood of healthy volunteers are shown in Table 4.5.

Table 4.4. Enantioanalysis of arginine in whole blood and gastric tumor tissue samples collected from patients confirmed with gastric cancer.

Sample No.	3D enantioselective needle stochastic sensor based on MnPorph and NS-doped graphene	L-arginine (μmol L^{-1})	D-arginine (pmol L^{-1})
Whole Blood			
1	NS-Gr-2	72.16±0.04	4.00±0.02
	NS-Gr-1	71.64±0.03	3.99±0.03
2	NS-Gr-2	25.44±0.02	6.36±0.04
	NS-Gr-1	25.00±0.03	6.30±0.03
3	NS-Gr-2	20.74±0.03	3.46±0.02
	NS-Gr-1	21.13±0.04	3.40±0.02
4	NS-Gr-2	19.26±0.03	2.19±0.03
	NS-Gr-1	20.29±0.03	2.36±0.02
5	NS-Gr-2	30.03±0.04	7.24±0.03
	NS-Gr-1	29.42±0.02	7.62±0.04
6	NS-Gr-2	11.39±0.03	6.20±0.02
	NS-Gr-1	11.78±0.02	6.15±0.03
7	NS-Gr-2	17.12±0.01	15.19±0.02
	NS-Gr-1	18.03±0.04	15.18±0.03
8	NS-Gr-2	18.39±0.03	1.93±0.02
	NS-Gr-1	19.04±0.03	1.96±0.01
9	NS-Gr-2	37.47±0.02	6.49±0.01
	NS-Gr-1	39.06±0.03	6.72±0.02
10	NS-Gr-2	16.30±0.01	4.80±0.03
	NS-Gr-1	16.28±0.03	4.83±0.02
11	NS-Gr-2	40.04±0.02	13.78±0.02
	NS-Gr-1	39.06±0.04	13.14±0.04
12	NS-Gr-2	75.46±0.02	8.06±0.03
	NS-Gr-1	75.40±0.03	8.21±0.04
13	NS-Gr-2	9.50±0.02	11.38±0.03
	NS-Gr-1	9.54±0.02	11.44±0.02
14	NS-Gr-2	32.37±0.03	8.71±0.03
	NS-Gr-1	32.00±0.02	8.39±0.04
15	NS-Gr-2	3.50±0.03	2.90±0.03
	NS-Gr-1	3.41±0.04	2.92±0.02
16	NS-Gr-2	82.97±0.02	7.38±0.01
	NS-Gr-1	83.69±0.03	7.25±0.01
17	NS-Gr-2	16.05±0.02	25.90±0.03
	NS-Gr-1	16.00±0.02	25.84±0.02
18	NS-Gr-2	10.93±0.03	14.52±0.02
	NS-Gr-1	10.90±0.02	15.64±0.02
19	NS-Gr-2	12.93±0.03	8.11±0.01

	NS-Gr-1	12.92±0.02	7.49±0.02
Gastric Tumoral Tissue			
1	NS-Gr-2	139.23±0.03	2.95±0.01
	NS-Gr-1	140.10±0.02	2.98±0.01
2	NS-Gr-2	127.98±0.02	2.62±0.03
	NS-Gr-1	124.04±0.02	2.64±0.02
3	NS-Gr-2	115.98±0.02	2.74±0.04
	NS-Gr-1	118.99±0.01	2.80±0.02
4	NS-Gr-2	116.03±0.01	10.39±0.03
	NS-Gr-1	116.47±0.01	9.28±0.02
5	NS-Gr-2	153.00±0.04	17.63±0.03
	NS-Gr-1	152.00±0.02	17.02±0.02
6	NS-Gr-2	143.07±0.01	3.40±0.01
	NS-Gr-1	142.96±0.04	3.49±0.02
7	NS-Gr-2	185.95±0.02	8.50±0.03
	NS-Gr-1	186.38±0.03	8.42±0.02
8	NS-Gr-2	159.14±0.01	7.05±0.02
	NS-Gr-1	160.04±0.02	6.16±0.03
9	NS-Gr-2	385.15±0.03	23.97±0.03
	NS-Gr-1	384.24±0.04	20.98±0.02
10	NS-Gr-2	146.93±0.02	12.83±0.01
	NS-Gr-1	147.88±0.03	12.80±0.02
11	NS-Gr-2	115.02±0.04	23.38±0.01
	NS-Gr-1	114.12±0.02	23.33±0.02
12	NS-Gr-2	132.74±0.04	5.42±0.01
	NS-Gr-1	133.93±0.03	5.27±0.02
13	NS-Gr-2	156.57±0.02	10.11±0.02
	NS-Gr-1	157.40±0.02	10.13±0.03

Table 4.5. Enantioanalysis of arginine in whole blood samples collected from healthy volunteers.

Sample No.	3D enantioselective needle stochastic sensor based on MnPorph and NS doped graphene	L-arginine (mol L^{-1})
1	NS-Gr-2	13.29±0.02
	NS-Gr-1	13.30±0.03
2	NS-Gr-2	17.40±0.02
	NS-Gr-1	17.79±0.01
3	NS-Gr-2	15.50±0.03
	NS-Gr-1	15.48±0.02
4	NS-Gr-2	16.50±0.01
	NS-Gr-1	16.53±0.02
5	NS-Gr-2	59.95±0.02
	NS-Gr-1	60.03±0.01

Very good correlations were recorded for the concentration of the enantiomers of arginine determined using the sensors based on NS-Gr-2 and NS-Gr-1. Furthermore, only the L-arginine was found in the whole blood of healthy patients proving that D-arginine may be a biomarker for the early detection of gastric cancer, making a differentiation between gastric cancer and gastric ulcer.

For further validation of the proposed 3D enantioselective needle stochastic sensors, synthetic solutions containing both enantiomers of arginine were prepared and the concentrations of the enantiomers were determined. The results are shown in Table 4.6.

Table 4.6. Recovery of the enantiomers of arginine when in different ratios.

3D enantioselective needle stochastic sensor based on MnPorph and N, S-doped graphene	L:D (mol:mol)	%, Recovery	
		L-arginine	D-arginine
NS-Gr-1	1:1	99.95±0.03	99.98±0.02
	1:2	99.99±0.01	99.97±0.02
	2:1	99.97±0.03	99.97±0.02
	1:10	99.95±0.02	99.99±0.03
	10:1	99.98±0.02	99.97±0.02
NS-Gr-2	1:1	99.93±0.03	99.95±0.04
	1:2	99.95±0.02	99.95±0.03
	2:1	99.97±0.01	99.96±0.03
	1:10	99.98±0.02	99.96±0.03
	10:1	99.98±0.01	99.95±0.03

Table 4.6 shows very high recoveries of L- and D-arginine, despite the ratio in which they were mixed, proving that they can be recovered with high reliability from mixtures, and that the proposed screening method can be validated for the enantioanalysis of arginine.

Compare with other sensors used for the assay of arginine to date (Table 4.7), the proposed sensor exhibited lower limits of determination than those reported earlier, and are able to discriminate between L- and D-enantiomers of arginine, while the others are not able to discriminate between the enantiomers of arginine.

Table 4.7 Comparison between the limits of determination of the sensors proposed to date, and the sensors used in this publication for the enantioanalysis of arginine.

Sensor	Limit of quantification, (mol L^{-1})	Ref
Potentiometric biosensor	5.0×10^{-4}	[162]
Amperometric biosensor based on urease	7.0×10^{-5}	[163]
Amperometric biosensor based on yeast cells/urease	1.5×10^{-4}	[164]
Arginine enzymatic sensor	5.0×10^{-4}	[165]
3D enantioselective needle stochastic sensor based on MnPorph and N, S-doped graphene 1	L-Arg: 1.0×10^{-15} D-Arg: 1.0×10^{-15}	This work
3D enantioselective needle stochastic sensor based on MnPorph and N, S-doped graphene 2	L-Arg: 1.0×10^{-14} D-Arg: 1.0×10^{-14}	This work

Chapter 5: 2D Enantioselective Disposable Stochastic Sensor for Fast Real Time Enantioanalysis of Glutamine in Biological Samples

5.3.1 Response Characteristics of the 2D Enantioselective Stochastic Sensor

Chronoamperometry made at the constant potential of 174 mV vs Ag/AgCl was employed for all measurements. When the potential was applied, the enantiomers went to the electrode interface, and got inside the channel – while entering the channel, the intensity of the current becomes zero (the time needed to enter the channel is called the signature of the enantiomer, and it is marked in the diagrams as t_{off}). While in the channel, the enantiomers undergo binding and redox processes – the time needed to complete the processes is marked on the diagram as t_{on}, and it is read in between two t_{off} values.

For the assay of L-glutamine the following response characteristics were obtained, when calibration was done in clean buffer solutions: signature of L-glutamine (t_{off} value) 1.4±0.1s, linear concentration range: $1x10^{-13}$-$1x10^{-3}$mol L^{-1}, limit of quantification $1x10^{-13}$mol L^{-1}, sensitivity: $1.72x10^{10}$ s^{-1} mol^{-1} L, equation of calibration: $\frac{1}{t_{on}} = 0.28 + 1.72 \times 10^{10} C$ (<t_{on}>=s; <C>=mol L^{-1}) with r=0.9996. When the calibration was repeated in the whole blood from a healthy volunteer, the calibration graph was: $\frac{1}{t_{on}} = 0.30 + 1.74 \times 10^{10} C$ (<t_{on}>=s; <C>=mol L^{-1}) with r=0.9999, and a sensitivity of $1.74x10^{10}$ s^{-1} mol^{-1} L; the linear concentration range and the limit of quantification did not change, when using whole blood for calibration.

For the assay of D-glutamine the following response characteristics were obtained when calibration was done in clean buffer solutions: signature of D-glutamine (t_{off} value) 0.3±0.1s, linear concentration range: $1x10^{-15}$-$1x10^{-3}$mol L^{-1}, limit of quantification $1x10^{-15}$mol L^{-1}, sensitivity: $1.17x10^{13}$ s^{-1} mol^{-1} L, equation of calibration: $\frac{1}{t_{on}} = 0.26 + 1.17 \times 10^{13} C$ (<t_{on}>=s; <C>=mol L^{-1}) with r=0.9998. When the calibration was repeated in the whole blood from a healthy volunteer, the calibration graph was: $\frac{1}{t_{on}} = 0.20 + 1.20 \times 10^{13} C$ (<t_{on}>=s; <C>=mol L^{-1}) with r=0.9999, and a sensitivity of $1.20x10^{13}$ s^{-1} mol^{-1} L; the linear concentration range and the limit of quantification did not change, when using whole blood for calibration.

Differences in the signatures' values proved that the sensor is enantioselective, the two enantiomers being able to be determined simultaneously in the biological samples. High sensitivities values were recorded, and low limits of determination, making possible their assay in healthy people, but also in patients with gastric cancers in different stages.

Reproducibility studies were performed as following: 10 sensors were manufactured following the procedure shown in Sensor Design paragraph. Each of the sensors was evaluated in the same way, and the sensitivities were determined and compared when immersed in L- and D-glutamine solutions. The RSD (%) values recorded for the sensitivities were: for the L-glutamine assay 0.10%, and for D-glutamine assay 0.11%. The RSD (%) values recorded for the sensitivities proved the reproducibility of the sensors design.

The stability of each 2D sensor (designed for single utilization) was checked as following: 10 sensors of each type were stored as described in the Sensors Design paragraph. Every day a different sensor was taken from the storage space and it was immersed in the solutions contain L- and D-glutamine of different concentrations; the sensitivities of each measurement was retained for comparison after the whole lot of sensors was consumed, in 30 days. The results recorded at the end of the period showed the high stability of the electrodes in time because the variation of the sensitivities in time were less than 0.50%.

5.3.2 The Selectivity and Enantioanalysis of the 2D Stochastic Sensor

The selectivity and enantioselectivity are given by the signatures of the enantiomers and analytes found in the real samples; a difference in the signatures' values shown that the proposed sensor is enantioselective and selective. The signatures of the analytes did not depend on the matrix from where the analytes are determined, but depend on: stereochemistry of the enantiomers; on the length and volume of the molecules, on their velocity to move inside the channel. Accordingly, all the analytes from a solution are getting inside the channel in a certain sequence, ordered by the length and stereochemistry of the molecules. Different signatures (t_{off} values) were recorded for L- and D-glutamine using the same 2D sensor (Table 5.1); this proved the enantioselectivity of the sensor. For the assessment of the selectivity, other amino acids such as tryptophan (try), proline (pro), and arginine (arg), were selected. Different signatures were obtained for those amino acids when compared with the signatures recorded for L- and D-glutamine, proving that the 2D sensors are also selective (Table 5.1).

Table 5.1. Selectivity of the 2D disposable stochastic sensors (N=10).

	Signature, t_{off} (s)							
Interferent	L-gln	D-gln	L-try	D-try	L-pro	D-pro	L-arg	D-arg
-	0.7±0.1	1.9±0.1	2.2±0.1	1.2±0.1	2.0±0.1	2.5±0.2	3.1±0.1	3.5±0.1

The values recorded for the signatures are reliable, being dependent on the size and geometry of the tested amino acid.

5.4 Enantioanalysis of Glutamine in Whole Blood and Tumor Tissue Samples

Whole blood and tissue samples were taken from confirmed patients with gastric cancer. Whole blood samples were obtained from healthy patients. The biological samples were analyzed as taken from the patients, according to the stochastic method described above.

The accuracy of the screening tests using the 2D enantioselective stochastic sensors was proved by standard addition of L- and D-glutamine to the biological samples. Recovery tests of L- and D-glutamine in the samples were performed as following: L- and D-glutamine were initially determined from the samples, and after that, known amounts of L- and D-glutamine were added. The recovered amounts of L- and D-glutamine were compared with those added to the whole blood sample.

Table 5.2 shows the results obtained for 10 whole blood samples and 10 gastric tumor tissue samples. The samples were screened accordingly with the stochastic method described above using the 2D enantioselective stochastic sensor. L- and D-glutamate were identified in the samples based on their signatures, t_{off} values (Figure 5.3). The concentrations of the enantiomers of glutamine were determined using the equations of calibrations for each enantiomer, after measuring in the diagrams (Figure 5.3) the values of t_{on} (these values are measured in between two consecutive t_{off} values – see Figure 5.3) for each enantiomer. The results showed that both L- and D-glutamine were found in the whole blood and gastric tumor tissues of the confirmed patients with gastric cancer (Table 5.2).

Table 5.2. Enantioanalysis of glutamine in whole blood and gastric tumor tissue samples of confirmed patients with gastric cancer.

Sample no.	Enantiomer of glutamine*	Glutamine, μmol L^{-1}	Enantiomeric excess (%)
Whole blood			
1	L	2.04±0.03	61.26
	D	0.49±0.02	
2	L	5.84±0.04	89.33
	D	3.29(±0.02) x10^{-1}	
3	L	2.13±0.02	58.07
	D	5.65(±0.03) x10^{-1}	
4	L	1.76±0.02	34.04
	D	8.66(±0.02) x10^{-1}	
5	L	2.35±0.03	99.73
	D	3.22(±0.01) x10^{-3}	
6	L	2.26±0.03	62.01
	D	0.53±0.03	
7	L	1.06±0.01	92.17
	D	4.32(±0.03) x10^{-2}	
8	L	4.37±0.04	90.79
	D	2.11(±0.02) x10^{-1}	
9	L	1.05±0.01	95.28
	D	2.54(±0.02) x10^{-2}	
10	L	5.84±0.03	91.70
	D	2.53(±0.01) x10^{-1}	
Gastric tumor tissue			
1	L	1.05±0.01	56.72
	D	0.29±0.02	
2	L	1.33±0.03	69.32
	D	2.41(±0.02) x10^{-1}	
3	L	1.66±0.02	86.83

	D	1.17(±0.03) x10^{-1}	
4	L	5.83±0.02	64.69
	D	1.25±0.03	
5	L	2.04±0.04	88.37
	D	1.26(±0.02) x10^{-1}	
6	L	1.06±0.02	3.64
	D	1.14±0.03	
7	L	1.33±0.02	59.47
	D	3.38(±0.03) x10^{-1}	
8	L	3.75±0.03	92.21
	D	1.52(±0.02) x10^{-1}	
9	L	1.06±0.03	3.41
	D	0.99±0.02	
10	L	7.51±0.02	95.62
	D	1.68(±0.03) x10^{-1}	

*All results are the average of 5 measurements.

Table 5.3. Enantioanalysis of glutamine in whole blood samples of healthy volunteers.

Sample no.	**Enantiomer of glutamine***	**L-glutamine, mmol L^{-1}**
1	L	0.46±0.02
2	L	0.30±0.02
3	L	0.26±0.01
4	L	0.13±0.02
5	L	0.11±0.01

*All results are the average of 5 measurements.

Whole blood samples from healthy patients were collected and analyzed using the stochastic sensors; the results of the enantioanalysis showed that only the L enantiomer of glutamine was found in the healthy patients, no D-glutamine was identified in the whole blood of the healthy

patients (Table 5.3). Further, the enantiomeric excess may be a trade mark for the evolution of illness.

Compared with the results obtained by Meyerhoff et al. [187] using a biosensor for the assay of L-glutamine as detector in flow injection analysis, the proposed 2D enantioselective stochastic sensor can be designed easier than the biosensor, no special storage conditions are required for the stochastic sensor compared with the biosensor that must be kept at 4°C, the biosensor had very low stability in time, the linear concentration range is wider for the stochastic sensor compared with the biosensor ($1x10^{-4}$ - $1x10^{-2}$mol L^{-1}), with a higher limit of determination for the biosensor compared with the stochastic sensor. The biosensor can only determine the L-glutamine, while the stochastic sensor can determine in the same run both enantiomers of glutamine.

Chapter 6: Stochastic Sensors Used in Pattern Recognition and Quantification of Maspin in Biological Samples

6.2.1.4 Design of the Stochastic Microsensors

The NS co-doped graphene (NSGR) powder was mixed with paraffin oil: 100mg powder was mixed with 30μL paraffin oil until a homogeneous paste was obtained. The paste was divided into two equal quantities and to each of them, a different modifier was added: to the first part, 50μL of a $1x10^{-3}$mol L^{-1} α-cyclodextrin solution was added, while to the second one, 50μL of a $1x10^{-3}$mol L^{-1} maltodextrin solution was added. Silver wire served as contact between the paste and the external circuit (Figure 6.1). Each modified paste was placed in non-conducting plastic tubes with inner diameter of 150μm, and a length of 5mm. The stochastic microsensors were washed with deionized water, and dried between measurements. When not in use, they are kept in a dry place.

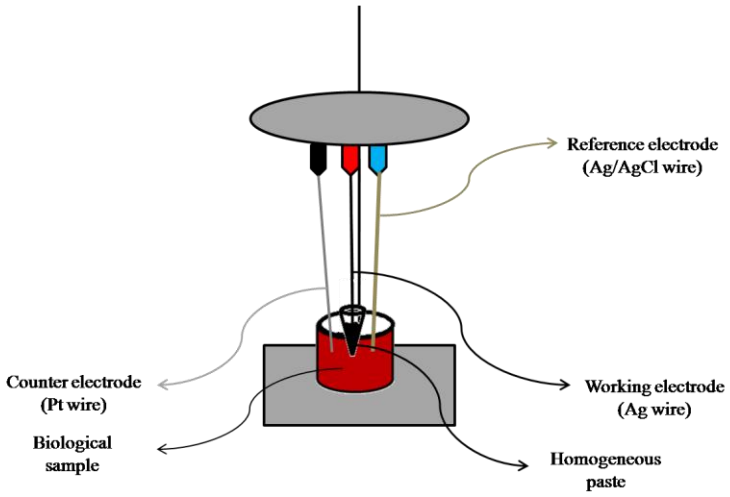

Figure 6.1. Diagram of the experimental set-up of the electrochemical cell.

6.2.1.5 Recommended procedures: Stochastic Method

All measurements were carried out at 25°C. A chronoamperometric method was used for the measurements of t_{on} and t_{off} at a constant potential (125 mV vs Ag/AgCl). Based on the value of t_{off}, the analyte was identified in the diagrams recorded with the stochastic microsensors and further the value of t_{on} was read and used for the determination of concentration (Figures 6.2-6.5). The unknown concentrations of maspin were determined from the calibration graphs $1/t_{on} = a + bxC_{maspin}$ recorded with each of the sensors for maspin.

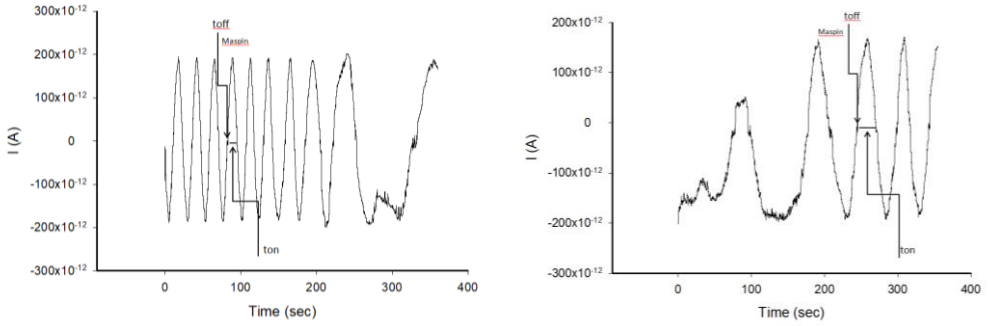

a b

Figure 6.2. Pattern recognition of maspin in whole blood samples, using stochastic microsensors based on NSGR and a) α-cyclodextrin, and b) maltodextrin.

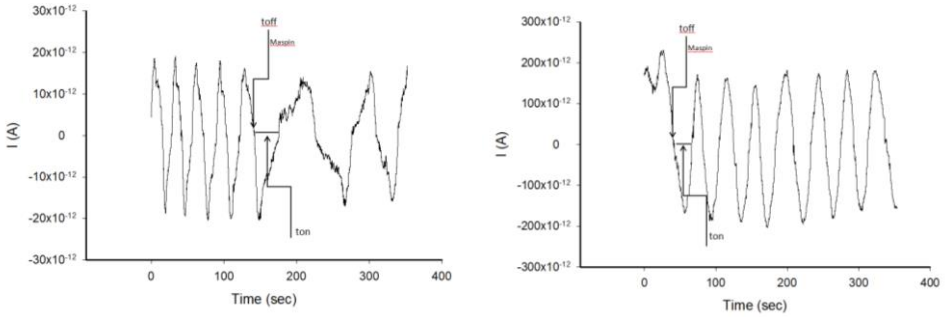

a b

Figure 6.3. Pattern recognition of maspin in saliva samples, using stochastic microsensors based on NSGR and a) α-cyclodextrin, and b) maltodextrin.

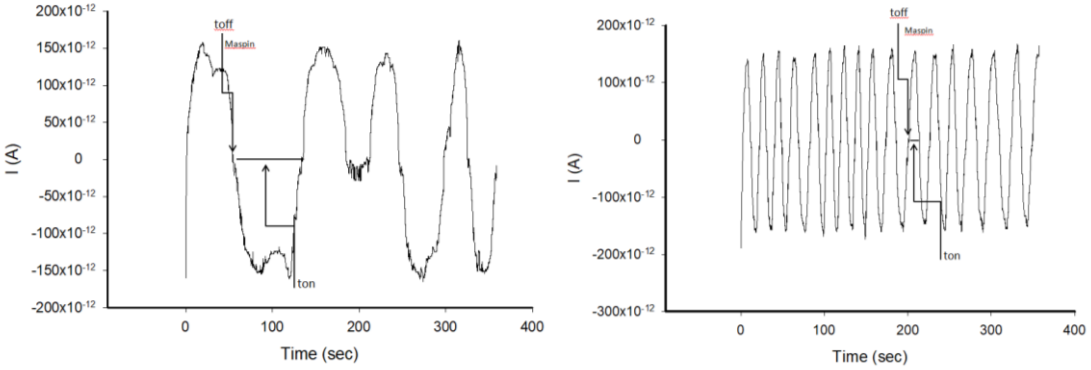

a b

Figure 6.4. Pattern recognition of maspin in urine samples, using stochastic microsensors based on NSGR and a) α-cyclodextrin, and b) maltodextrin.

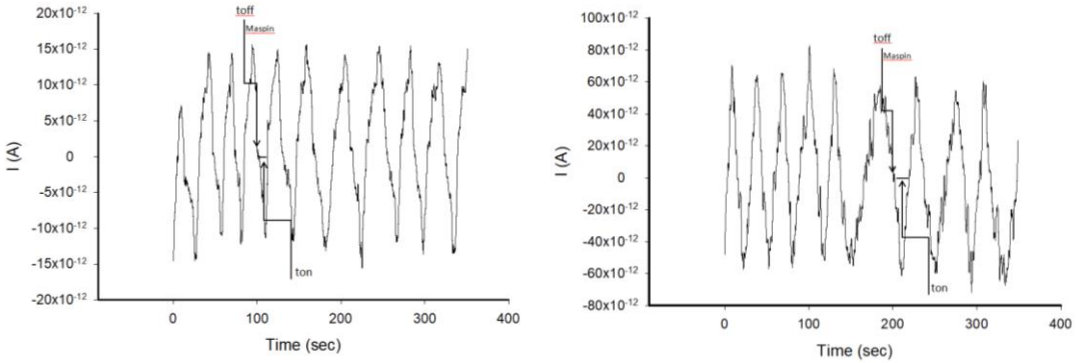

a b

Figure 6.5. Pattern recognition of maspin in tissue samples, using stochastic microsensors based on NSGR and a) α-cyclodextrin, and b) maltodextrin.

6.2.1.6 Samples

The biological samples such as: whole blood, gastric tumor tissue, saliva and urine were obtained from the Hospital of Targu Mures (Ethics committee approval no. 75/2015). These samples were obtained from confirmed patients with gastric cancer as well as from healthy patients. The patients were not under any treatment for gastric cancer before gathering the samples. The biological samples did not require any pretreatment before the measurements. The electrochemical cell was loaded up with the biological sample, and after recording the diagram, and identifying the signature of the maspin, the unknown concentrations of the biomarkers in entire biological tests were determined utilizing the stochastic method shown above.

6.2.2 Results and Discussions

6.2.2.1 Morphological and Structural Characterization of NSGR Sample

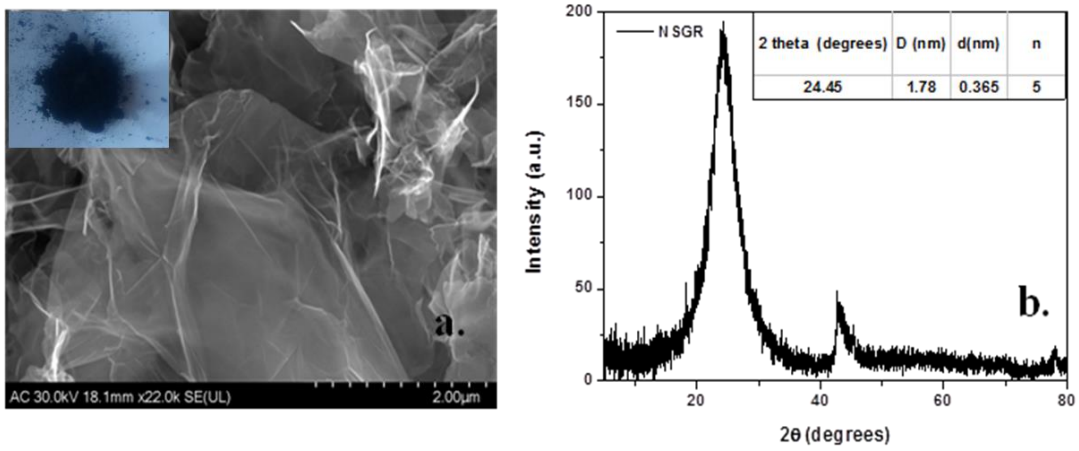

Figure 6.6. SEM (a) and XRD (b) of NSGR sample

In Fig. 6.6a is shown a representative SEM micrograph of NS co-doped graphene sample. Macroscopically, the sample is a black powder composed of large flakes (see the inset). Microscopically, the graphene flakes are thin and transparent with the lateral size of few micrometers. The basal plane of graphene sheet appears as smooth area of grey color while the edges of graphene appear as bright lines.

The corresponding XRD pattern presented in Fig. 6.6b reveals a relatively broad peak centered at about 24°, due to the (002) reflections, thus confirming the graphene structure of the prepared material. The calculated structural parameters from the recorded data are presented in the inset of Fig. 6b: the size of graphene crystallites (D) is around 1.78 nm with an interlayer distance (d) of 0.365 nm. In addition, the graphene crystallites are very thin, being composed of few-layers (n= 5).

6.2.2.2 Response Characteristics of the Stochastic Sensors

The response characteristic of the stochastic sensors is based on channel conductivity: after applying a potential of 125mV, the biomarker molecule enters in the channel blocking it while the intensity of the current drop to 0 A. The time spent for this type of stage is called the signature of the maspin. In the next stage, the maspin undergo binding processes as well as redox processes – the time spent for these processes being known as t_{on} – and it is used for quantitative measurements. Response characteristics of the stochastic microsensors were determined at two pHs, with the values 7.40, and 3.00, because we need to use the microsensors for assay of maspin in whole blood, gastric tumor tissues, and saliva (pH 7.40), and urine (pH 3.00). The response characteristics of the proposed microsensors are shown in Table 6.1.

Table 6.1. Response characteristics of stochastic microsensors used for the assay of maspin.

Stochastic microsensor based on NSGR and on	**Calibration equation* and correlation coefficient (r)**	**Linear concentration range ($g \cdot mL^{-1}$)**	**t_{off} (s)**	**Sensitivity ($s^{-1}/g \cdot mL^{-1}$)**	**Limit of quantification ($g \cdot mL^{-1}$)**
pH=7.40					
Maltodextrin	$1/t_{on}=0.03+2.95x10^{4}xC$ r=0.9998	$4.10x10^{-14}$ – $2.00x10^{-6}$	3.6	$2.95x10^{4}$	$4.10x10^{-14}$
α-Cyclodextrin	$1/t_{on}=0.03+3.82x10^{4}xC$ r=0.9999	$4.10x10^{-14}$ – $2.00x10^{-6}$	2.8	$3.82x10^{4}$	$4.10x10^{-14}$
pH=3.00					
Maltodextrin	$1/t_{on}=0.03+9.68x10^{2}xC$ r=0.9999	$1.02x10^{-12}$ – $8.00x10^{-7}$	3.4	$9.68x10^{2}$	$1.02x10^{-12}$
α-Cyclodextrin	$1/t_{on}=0.04+2.96x10^{3}xC$ r=0.9995	$2.05x10^{-13}$ – $2.00x10^{-6}$	2.8	$2.96x10^{3}$	$2.05x10^{-13}$

*$<1/t_{on}> = s^{-1}$ $<C> = g \cdot mL^{-1}$

For the pH 7.40, the highest sensitivity (the slope of the equation of calibration, $3.82x10^{4}$ $s^{-1}/g \cdot mL^{-1}$) was recorded when α-cyclodextrin was used as modifier, while the linear concentration range and the limit of quantification remain the same for both stochastic microsensors. The limit of quantification (considered the lowest value of concentration from the linear concentration range) at pH 7.40 is very low ($4.10x10^{-14}$ $g \cdot mL^{-1}$). For the pH 3.00, the highest sensitivity ($2.96x10^{3}$ $s^{-1}/g \cdot mL^{-1}$) as well as the lowest limit of quantification ($2.05x10^{-13}$ $g \cdot mL^{-1}$), and the widest linear concentration range ($2.05x10^{-13}$ – $2.00x10^{-6}$ $g \cdot mL^{-1}$) was obtained for the microsensor based on α-

cyclodextrin. Accordingly, the stochastic microsensor based on α-cyclodextrin is the microsensor of choice. The proposed stochastic microsensors were used for a period of 6 months, during which no significant changes were observed in terms of sensitivity.

6.2.2.3 Selectivity

The selectivity of the stochastic microsensors is given by the signatures (t_{off} values) of the maspin and of the possible interfering species; differences between the signatures means that the microsensors are selective. The interfering species selected were: p53, CEA, and CA19-9.

Table 6.2. Selectivity of the stochastic microsensors used for the determination of maspin.

Stochastic microsensor based on NSGR and on	Maspin, Signature (s)	CEA, Signature (s)	CA19-9, Signature (s)	p53, Signature (s)
pH=7.40				
Maltodextrin	3.6	2.4	0.5	1.2
α-Cyclodextrin	2.8	1.8	1.2	0.5
pH=3.00				
Maltodextrin	3.4	2.1	1.3	0.8
α-Cyclodextrin	2.8	1.8	1.1	3.2

The results shown in Table 6.2 proved that CA, CA19-9, and p53 did not interfere in the determination of maspin at either pH 7.40 or pH 3.00.

6.2.3 Pattern Recognition and Determination of Maspin in Biological Samples

Samples like whole blood, gastric tumor tissue, saliva and urine from patients confirmed with gastric cancer as well as whole blood samples donated by healthy people were screened using the two stochastic microsensors. Pattern recognition was done first – based on the identification of the t_{off} value (signature) specific to maspin in the diagrams obtained using the proposed stochastic microsensors. Just after reading the t_{off} value, in between two t_{off} values, the corresponding t_{on}

values were read. The t_{on} values were used to determine the concentrations of maspin in the biological samples, accordingly with the stochastic method described above.

The first step of validation was the recovery test – which was done for each of the biological samples (whole blood, gastric tumor tissue, saliva, urine) by addition of well-known amounts of maspin, and determination using the proposed sensors the % recovery in each of the biological sample. Results of the recovery test are shown in Table 6.3.

Table 6.3. Recovery tests of maspin in biological samples using the stochastic microsensors (N=10).

Stochastic microsensor based on NSGR and on	**Maltodextrin**	**α-cyclodextrin**
Type of sample	Maspin, Recovery, %	
Whole blood	97.89±0.03	99.87±0.02
Gastric tumor tissue	97.33±0.04	99.47±0.02
Saliva	97.14±0.04	99.12±0.03
Urine	98.83±0.03	99.89±0.03

High recoveries, and low RSD values (lower than 0.10%) were recorded in the recovery tests.

The second validation step was done by pattern recognition and determination of maspin in whole blood, gastric tumor tissue, saliva, urine. Part of the results obtained are shown in Table 6.4.

Table 6.4. Results obtained for the quantification of maspin in biological samples, using the stochastic microsensors (N=10).

Stochastic microsensor based on NSGR and on	Maspin, ng mL^{-1}		
Sample No.	Maltodextrin	α-Cyclodextrin	ELISA
Whole blood from confirmed patients with gastric cancer			
1	0.39±0.03	0.38±0.02	0.40
2	0.20±0.02	0.23±0.01	0.24
3	0.30±0.01	0.31±0.03	0.32
4	0.15±0.02	0.16±0.03	0.16
5	0.13±0.02	0.13±0.02	0.15
t-test	2.73	1.83	-
Whole blood from healthy volunteers			
1	6.21±0.03	6.48±0.03	6.82
2	6.09±0.01	5.92±0.04	6.30

3	9.93±0.03	9.22±0.04	10.02
4	2.35±0.01	2.18±0.03	2.40
5	2.37±0.03	2.03±0.02	2.57
t-test	2.75	1.80	-
Gastric tumor tissue sample			
1	0.48±0.03	0.48±0.02	0.50
2	0.30±0.02	0.33±0.03	0.35
3	0.17±0.02	0.18±0.01	0.17
4	0.17±0.01	0.18±0.03	0.19
5	0.23±0.03	0.21±0.02	0.24
t-test	2.58	2.90	-
Saliva			
1	0.42±0.03	0.45±0.02	0.45
2	0.22±0.02	0.25±0.03	0.26
3	0.70±0.03	0.69±0.04	0.70
4	0.32±0.02	0.38±0.03	0.37
5	0.39±0.03	0.39±0.02	0.40
t-test	2.14	1.89	-
Urine			
1	6.59±0.03	6.87±0.02	6.90
2	2.93±0.04	2.67±0.03	2.70
3	7.31±0.02	7.54±0.03	7.55
4	2.37±0.02	2.94±0.03	2.98
5	7.48±0.03	7.45±0.01	7.74
t-test	1.19	1.54	-

Very good correlations between the results obtained using the stochastic microsensors and ELISA (a standard kit used in accredited clinical laboratories). Paired t-test was also performed at 99.00% confidence level (tabulated theoretical t-value: 4.032) for each type of sample and microsensor, versus ELISA. All calculated t-values were less than 4.032 proving that there is no statistically significant difference between the results obtained using the proposed stochastic microsensors (Table 6.4). Accordingly, the proposed stochastic microsensors can be reliably used for the molecular recognition and quantification of maspin in the selected biological samples.

Both validation tests showed that the proposed stochastic microsensors can be reliably used for pattern recognition and quantification of maspin in biological samples.

6.3 Stochastic Sensors for Pattern Recognition and Quantification of Maspin

6.3.1 Experimental

6.3.1.3 Design of the Disposable Stochastic Sensors

The composite material thin films were deposited using a mixture of graphene nanoplatelet (GNPs) and silver particles (AgPs) as precursor. The steps of the design are shown in Scheme 6.1.

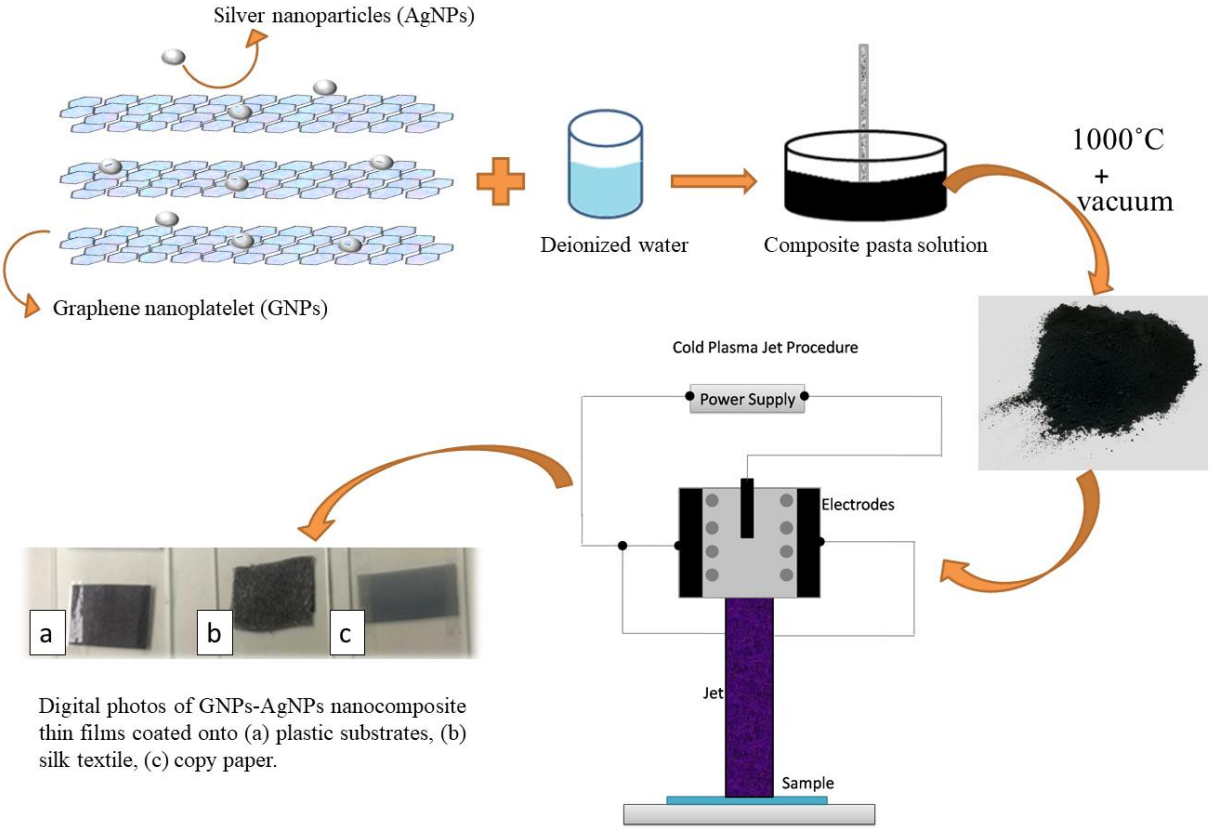

Scheme 6.1. Deposition of materials on plastic, silk textile, and copy paper using cold plasma.

The materials were manually mixed in double deionized (DI) water in order to obtain a pasta solution. 4 g of GNPs from Nanografi (No: 7782-42-5) and 2 g of AgPs (99.9 %) with different dimensions in the size range of 30-60 µm were mixed in 10 mL of DI. The composite pasta solution was baked at 1000° C for 1 h in high vacuum, resulting in a solid target which used as precursor for the coating process. A cold plasma source developed in our laboratory, called Thermionic

Vacuum Arc, was used for coating. Plastic, silk and paper placed above the plasma source at a distance of 27 cm were used as substrates and the deposition was carried out for 20 minutes under high vacuum conditions (1.3 x10^{-5}mBar). The electrical parameters of plasma were: 53 A filament current, 1.8 A plasma current and 200 V plasma voltage.

It is obvious that the GNPs-AgNPs nanocomposite thin film proposed in this work are uniformly coated on the organic substrates. Images revealed that the coated substrates have a rough surface, with many irregularly of round nanoclusters.

Over the working electrode a solution of chitosan (10^{-5} mol L^{-1}) was dropped; after that, the sensor was left to dry for 24h. The sensors were stored in dry places, at room temperature.

6.3.1.4 Stochastic Method

For the stochastic mode, a chronoamperometric technique was selected, for which a constant potential (125 mV versus Ag/AgCl) was applied. This method was used for both the qualitative and the quantitative analysis of maspin from whole blood, saliva, urine and tissue samples from confirmed patients with gastric cancer. Two parameters were identified, t_{off} and t_{on} respectively, from the stochastic diagrams (Figures 6.7-6.10).

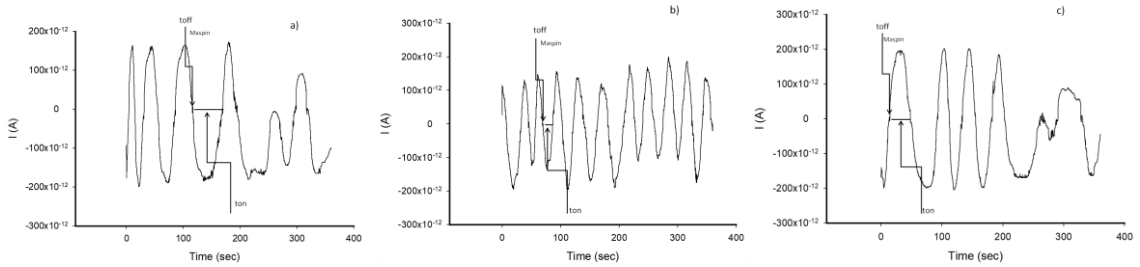

Figure 6.7 Examples of diagrams obtained for the screening tests of whole blood using the disposable stochastic sensors based on chitosan and GNPs-AgNPs immobilized on (a) silk; (b) copy paper; (c) plastic.

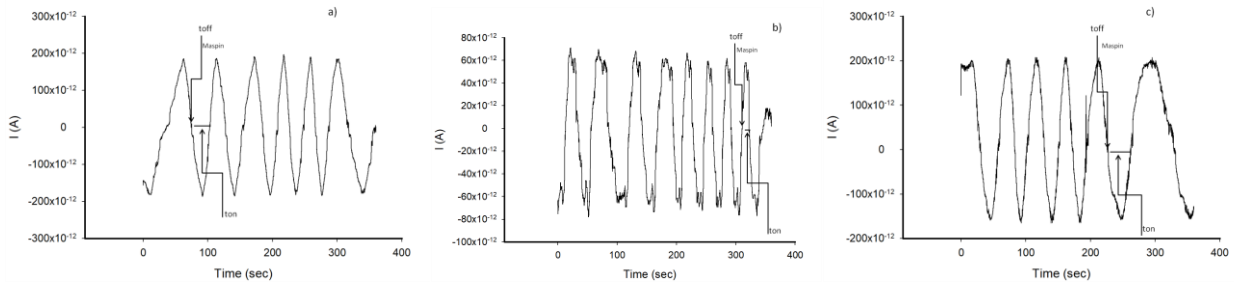

Figure 6.8. Examples of diagrams obtained for the screening tests of saliva using the disposable stochastic sensors based on chitosan and GNPs-AgNPs immobilized on (a) silk; (b) copy paper; (c) plastic.

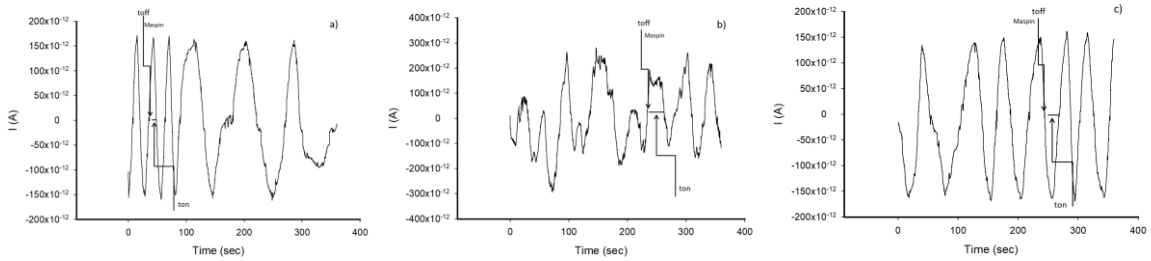

Figure 6.9. Examples of diagrams obtained for the screening tests of urine using the disposable stochastic sensors based on chitosan and GNPs-AgNPs immobilized on (a) silk; (b) copy paper; (c) plastic.

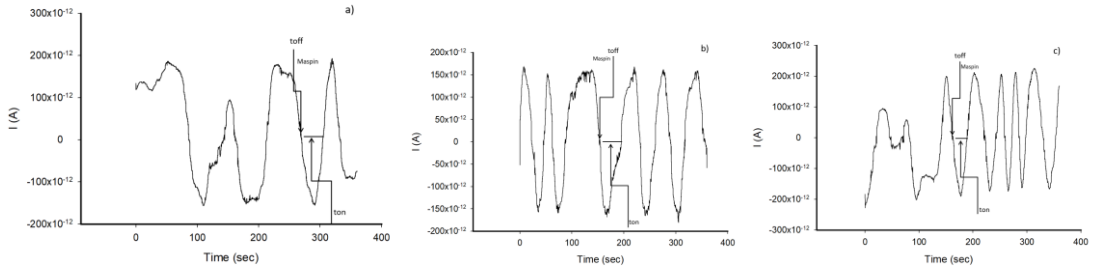

Figure 6.10. Examples of diagrams obtained for the screening tests of tumoral tissues using the disposable stochastic sensors based on chitosan and GNPs-AgNPs immobilized on (a) silk; (b) copy paper; (c) plastic.

t_{off} is known as the signature of the analyte and its value is used for the qualitative analysis; based on its value, the maspin was identified in the diagrams obtained for the analysis of biological samples (Figures 6.7-6.10). After that, the t_{on} value was read (this is known as the necessary time of equilibrium for the interaction of the analyte with the wall channel and redox processes) and it represents the quantitative parameter ($1/t_{on} = a+bxC_{maspin}$). The equations of calibration were obtained by using the linear regression method. Calibrations were performed for all disposable sensors at two pH values: 3.00, and 7.40.

6.3.1.5 Samples

Biological samples such as: blood, tissue, saliva and urine obtained from confirmed patients with gastric cancer were analyzed. The patients were not under any treatment for gastric cancer

before the samples were gathered. These samples were obtained from the Hospital of Targu-Mures (ethics committee approval no. 75/2015). The analyzed biological samples did not need any processing before the measurement. The unknown concentrations of maspin in the biological samples were determined using the stochastic mode described above.

6.3.2 Results and Discussions

6.3.2.1 Response Characteristics of the Disposable Stochastic Sensors

The determination of the signature of maspin (t_{off}) value served for qualitative analysis in the diagrams obtained for the biological samples (Figures 6.7-6.10, Table 6.5), while the values of t_{on} were used for the determination of the response characteristics of the sensors (Table 6.5) as well as for the quantitative determination of maspin in the biological samples. The response characteristics were reported for two pH values: 3.00 and 7.40 (Tables 6.5); the reason of calibrating the sensors at two pHs is that we do not want to do any treatment of the biological sample before the measurements, and these two pHs covered the native pHs of the biological samples tested.

For both pHs, when silk was used as support material for the design of the disposable stochastic sensor, the highest sensitivities were obtained: $5.76x10^{2}$ $s^{-1}/g\ mL^{-1}$ for pH 7.40, and $7.13x10^{3}$ $s^{-1}/g\ mL^{-1}$ for pH 3.00. For the sensors designed using the silk as support material the wider linear concentration ranges were obtained: $5.12x10^{-12}$ – $2.00x10^{-6}g\ mL^{-1}$ for pH 7.40, and $4.10x10^{-14}$ – $2.00x10^{-6}g\ mL^{-1}$ for pH 3.00, with the lowest limits of quantification of: $5.12x10^{-12}$ g $mL^{-1}$for pH 7.40, and $4.10x10^{-14}$ g mL^{-1} for pH 3.00. A very low limit of quantification (the lower concentration from the linear concentration range) was also obtained when the copy paper was used as substrate ($5.12x10^{-12}$ g mL^{-1}) for measurements performed at pHs 7.40 and 3.00. Overall, the best material – as support was proved to be the silk – in terms of high sensitivity, and wideness of the linear concentration range.

Table 6.5. Response characteristics of the disposable stochastic sensors used for the analysis of maspin.

Disposable stochastic sensor based on chitosan and GNPs-AgNPs immobilized on	Calibration equation* and correlation coefficient (r)	Linear concentration range ($g \cdot mL^{-1}$)	t_{off} (s)	Sensitivity ($s^{-1}/g \cdot mL^{-1}$)	Limit of quantification ($g \cdot mL^{-1}$)
pH=7.40					
Silk	$1/t_{on}=0.01+5.76x10^{2}xC$ r=0.9998	$5.12x10^{-12} – 2.00x10^{-6}$	2.6	$5.76x10^{2}$	$5.12x10^{-12}$
Copy paper	$1/t_{on}=0.04+1.24x10^{2}xC$ r=0.9999	$5.12x10^{-12} – 8.00x10^{-7}$	2.8	$1.24x10^{2}$	$5.12x10^{-12}$
Plastic	$1/t_{on}=0.02+7.21x10^{-2}xC$ r=0.9999	$1.60x10^{-8} – 2.00x10^{-6}$	2.4	$7.21x10^{-2}$	$1.60x10^{-8}$
pH=3.00					
Silk	$1/t_{on}=0.06+7.13x10^{3}xC$ r=0.9999	$4.10x10^{-14} – 2.00x10^{-6}$	3.0	$7.13x10^{3}$	$4.10x10^{-14}$
Copy paper	$1/t_{on}=0.02+7.37x10^{2}xC$ r=0.9995	$5.12x10^{-12} – 2.00x10^{-6}$	2.8	$7.37x10^{2}$	$5.12x10^{-12}$
Plastic	$1/t_{on}=0.04+4.01x10^{3}xC$ r=0.9993	$2.04x10^{-13} – 8.00x10^{-7}$	2.2	$4.01x10^{3}$	$2.04x10^{-13}$

*$<1/t_{on}> = s^{-1}<C> = g \cdot mL^{-1}$

Reproducibility studies were performed for each type of sensor. In this regard, 10 sensors of each type were manufactured following the procedure shown in Sensor Design paragraph. Each of the sensors were evaluated in the same way, and the sensitivities were determined and compared when immersed in maspin solutions of pHs 3.00 and 7.40. The RSD (%) values recorded for the sensitivities were: for the sensors based on silk: 0.12% at pH 7.40, and 0.15% at pH 3.00; for the sensors based on copy paper: 0.10% at pH 7.40, and 0.17% at pH 3.00; and for the sensor based on plastic: 0.09% at pH 7.40 and 0.08% at pH 3.00. The RSD (%) values recorded for the sensitivities proved the reproducibility of the sensors design.

The stability of each 2D sensor (designed for single utilization) was checked as following: 60 sensors of each type were stored as described in the Sensors Design paragraph. Every day it was taken from the storage place another sensor which was immersed in solutions containg maspin of different concentrations, and at pHs 3.00 and 7.40; the sensitivities of each measurement was retained for comparison after the all lot of sensors was consumed, in 30 days. The results recorded at the end of the period shown a high stability of the electrodes in time because the variation of the sensitivities in time were: for the sensors based on silk: 0.06% at pH 7.40, and 0.03% at pH 3.00;

for the sensors based on copy paper: 0.05% at pH 7.40, and 0.03% at pH 3.00; and for the sensor based on plastic: 0.07% at pH 7.40 and 0.05% at pH 3.00.

6.3.2.2 Selectivity

The selectivity of the disposable stochastic sensors is given by the t_{off} values (signatures) recorded for different possible interferents. CEA, CA 19-9, p53, glucose, glutamine, and CA72-4 were checked as possible interferences, at both pHs: 7.40, and 3.00.

Table 6.6. Selectivity of the disposable stochastic sensors used for the analysis of maspin.

Disposable stochastic sensor based on chitosan and GNPs-AgNPs immobilized on	**Maspin, Signature (s)**	**CEA, Signature (s)**	**CA19-9, Signature (s)**	**p53, Signature (s)**	**Glucose, Signature (s)**	**Glutamine, Signature (s)**	**CA72-4, Signature (s)**
pH=7.40							
Silk	2.6	1.4	0.7	3.0	0.3	1.7	3.1
Copy paper	2.8	1.5	0.5	3.5	0.2	1.9	3.3
Plastic	2.4	1.5	0.8	3.2	0.2	1.8	2.7
pH=3.00							
Silk	3.0	1.7	0.5	2.3	1.0	0.7	2.8
Copy paper	2.8	1.8	0.4	2.1	0.7	1.3	2.8
Plastic	2.2	1.8	0.6	2.6	0.2	1.3	3.0

Table 6.6 shows that none of the selected substances interfere in the determination of maspin either at pH 7.40 or at pH 3.00, because, their signatures are different from the signature of maspin.

6.3.3 Molecular Recognition and Quantification of Maspin in Biological Samples

The three disposable stochastic sensors were used for the fast screening of biological samples: whole blood, gastric tumor tissues, urine, and saliva obtained from patients with gastric cancer, and of whole blood samples obtained from healthy volunteers. First of all, the maspin was identified in the diagrams (Figures 6.7-6.10) based on its signature, and then the corresponding t_{on} was read and used as described in the stochastic mode for the determination of the concentration

of maspin. The results for 5 samples of each category are shown in Table 6.7; more than 100 samples were analyzed; the t-test value is the one resulting after the analysis of all samples. There is a very good correlation between the results obtained using the disposable stochastic sensors and ELISA – which is the standard method used in accredited laboratories.

Table 6.7 Results obtained for the fast screening of biological samples using the disposable stochastic sensors (N=10).

Disposable stochastic sensor based on chitosan and GNPs-AgNPs immobilized on / **Sample No**	**Gender**	**Age**	**Copy paper**	**Silk**	**Plastic**	**ELISA**
Whole blood from confirmed patients with gastric cancer						
1	M	60	0.39±0.03	0.34±0.02	0.38±0.01	0.40±0.11
2	M	69	0.21±0.03	0.23±0.03	0.23±0.03	0.24±0.11
3	F	65	0.27±0.02	0.28±0.03	0.28±0.02	0.28±0.13
4	M	69	0.14±0.02	0.14±0.02	0.15±0.01	0.16±0.10
5	M	73	0.12±0.03	0.14±0.02	0.12±0.01	0.15±0.13
t-test			1.98	2.03	2.12	-
F-test			1.23	1.58	1.87	-
Whole blood from healthy volunteers						
1	M	25	6.74±0.03	6.41±0.02	6.94±0.03	6.82±0.14
2	M	76	6.50±0.03	6.36±0.02	6.25±0.04	6.30±0.14
3	M	68	9.31±0.02	9.67±0.03	9.40±0.05	10.02±0.13
4	F	60	2.17±0.04	2.85±0.03	2.88±0.03	2.90±0.11
5	M	83	2.14±0.03	2.59±0.02	2.51±0.03	2.57±0.11
t-test			2.03	1.97	2.05	-
F-test			1.66	1.85	1.96	-
Gastric tumor tissue sample						
1	M	60	0.48±0.02	0.49±0.03	0.50±0.03	0.50±0.12
2	M	69	0.27±0.03	0.25±0.04	0.26±0.03	0.27±0.12
3	F	65	0.15±0.01	0.16±0.03	0.16±0.02	0.17±0.13
4	M	69	0.14±0.01	0.15±0.02	0.15±0.03	0.15±0.13
5	M	73	0.26±0.03	0.25±0.02	0.23±0.01	0.24±0.12
t-test			2.12	2.35	2.05	-
F-test			1.40	1.57	1.23	-
Saliva						
1	M	60	0.45±0.03	0.46±0.03	0.47±0.02	0.47±0.12
2	M	69	0.28±0.03	0.29±0.04	0.26±0.03	0.27±0.14
3	F	65	0.68±0.03	0.69±0.02	0.65±0.03	0.70±0.14

4	M	69	0.34±0.02	0.31±0.03	0.31±0.04	0.32±0.12
5	M	73	0.40±0.04	0.41±0.03	0.41±0.02	0.40±0.11
t-test			2.19	2.22	2.27	-
F-test			1.23	1.48	1.17	-
Urine						
1	M	60	6.74±0.02	6.78±0.03	6.28±0.03	6.80±0.13
2	M	69	2.71±0.03	2.52±0.03	2.39±0.04	2.40±0.11
3	F	65	7.30±0.03	7.44±0.04	7.46±0.04	7.45±0.11
4	M	69	2.34±0.01	2.35±0.03	2.30±0.04	2.30±0.12
5	M	73	7.55±0.03	7.82±0.02	7.07±0.01	7.83±0.11
t-test			2.21	2.94	3.10	-
F-test			1.45	1.19	2.04	-

A paired student t-test was performed at 99.00% confidence level (tabulated theoretical t-value: 4.032). The t-values calculated for each of the sensors and each type of sample were less than 4.032; this result proved that there is no statistically significant difference between the results obtained using the proposed stochastic sensors (Table 6.7), and that the disposable stochastic sensors can be reliably used for the molecular recognition and quantification of maspin in the selected biological samples. An F-test was also performed for each screening test when the proposed sensors were used as screening tools. Since the calculated F values (Table 3) are less than the tabulated F value (6.39, at 95% confidence level), one concludes that there is no significant difference in the precision of the proposed screening method using the 2D stochastic sensors and ELISA (the standard deviations are from random error alone, and don't depend on sample).

Further, the validation was done using standard addition method which involved addition of well-known amounts of maspin in each type of biological sample: whole blood, tissue sample, urine, and saliva. The recovery tests of the known amounts are shown in Table 6.8.

Table 6.8 Recovery tests of maspin in biological samples using the disposable stochastic sensors (N=10).

Disposable stochastic sensor based on chitosan and GNPs-AgNPs immobilized on	**Copy paper**	**Silk**	**Plastic**
Type of sample	Maspin, Recovery, %		
Whole blood	97.45±0.05	99.47±0.03	98.98±0.03
Gastric tumor tissue	96.82±0.03	99.98±0.02	97.99±0.04
Saliva	98.03±0.03	99.00±0.04	98.85±0.02
Urine	98.13±0.03	99.21±0.03	99.07±0.03

Very high recovery values were obtained for maspin when determined from the four types of biological samples. These values proved further, that the proposed disposable stochastic sensors can be used for a reliable recognition and quantification of maspin in biological samples.

Chapter 7: Determination of p53 From Whole Blood Samples Using an Electrochemical Sensor Based on Graphene Decorated with N and S

7.1 Introduction

Cancer is a high mortality disease in modern society, and it's the cause of a high rate of all deaths globally [203]. Early-stage monitoring of cancer biomarkers is especially important for providing vital information of diagnostics and efficient and time-saving therapy.

The protein p53 is a well-known tumor suppressor that plays a vital role in the repairing of DNA, apoptosis and cell proliferation [204]. There are studies where it was demonstrated that in the case of mice, fully-developed mice that lack p53 protein suffers from different types of cancer; for humans, more than 50% of all cancers develops some sort of mutations in time [205,206]. Consequently, the accurate detection of cancer biomarker p53 protein is very important for the early diagnosis and efficient therapy of cancer. Due to the fact that, in more than half of the cases of cancers, the p53 protein suffers mutations, it was found that in the human sera the level of the protein is even low compared to the normal levels [206], and it was highly desirable to develop a sensitive, reliable and selective analytical technique for detecting p53 level.

To date, various techniques have been developed to determine protein biomarkers, for detection of p53 to date, best performances were achieved using surface plasmon resonance (SPR) [207], field-effect transistors [208], DNA probe techniques [209], including enzyme-linked immunosorbent assays (ELISA) [210], electrochemiluminescence (ECL) [211]. Among them, electrochemical techniques have been received wide attention due to their straightforward, high selectivity, and time-saving procedure [212-219].

In this paper we proposed an electrochemical sensor based on graphene decorated with N and S, modified with 2,3,7,8,12,13,17,18-octaethyl-21H,23H-porphirine manganese (III) chloride solution for the assay of p53 in whole blood samples.

7.2.3 Design of the Electrochemical Sensor

The paste used as active side of the electrochemical sensor was obtained by physical mixing 100 µL solution of 2,3,7,8,12,13,17,18-octaethyl-21H,23H-porphirine manganese (III) chloride (10^{-3} mol L^{-1}) with 100mg paste (obtained by mixing graphene decorated with N and S with paraffin oil). The modified paste was placed in a non-conducting polymer tube with an internal diameter of 150µm. Electric contact was made using a silver wire. Between the measurements, the sensor was washed with deionized water and dried. When not in use, the sensor was kept in a dry place at room temperature.

7.2.4 Recommended procedure

DPV was used for the measurements of each standard solution of known concentration (1.0 x 10^{-8} µg mL^{-1} – 5.00µg/mL). The working parameters were as following: scan rate was 90 mVs^{-1}, potential range -1 - 0.750 V, and modulation amplitude 50 mV. The equation of calibration (I=f ($Conc._{p53}$)) was obtained using linear regression method, and it was used for calculations of unknown concentrations of p53 in whole blood samples. The calibration graphic is presented in Figure 7.1.

7.2.5 Samples

Whole blood samples were obtained from the Clinical County Hospital of Targu Mures (Ethics committee approval nr. 75/2015) from 5 different patients diagnosed with gastric cancer. These samples were used for the direct assay of p53 without any pretreatment.

7.2.6 Selectivity Studies

The study of selectivity of the electrochemical sensor was done versus: CEA, L- and D-aspartic acid, and L- and D-glutamine. Mixed solution method was used for determining if there are any interferences. A ratio of 1:10 (mol/mol; p53: interferent) was considered when prepared the mixed solutions.

7.3 Results and Discussions

7.3.1 Characteristic Response of the Proposed Electrochemical Sensor

Differential pulse voltammetry (DPV) technique was used to determine the response characteristics of the proposed electrochemical sensor, when used for the assay of p53. The half wave potential was recorded at -351mV. The equation of calibration was:

$$I = 5.79x10^{-7} + 2.89x10^{-8}xC_{p53},$$

where I is the height of the peak in A, and C_{p53} is the concentration in μg mL^{-1}. The correlation coefficient, r is 0.9532. The sensitivity of the electrochemical sensor is $2.89x10^{-8}$A/μg mL^{-1}. The linear concentration range was between 8ng mL^{-1} and 5 μg mL^{-1}. The limit of detection was determined as 0.1ng mL^{-1}.

The results showed a good value of the sensitivity and a low limit of determination of p53. The proposed sensor covered the range on which p53 can be found on healthy people, as well as for patients presenting stages 1-3 of gastric cancer.

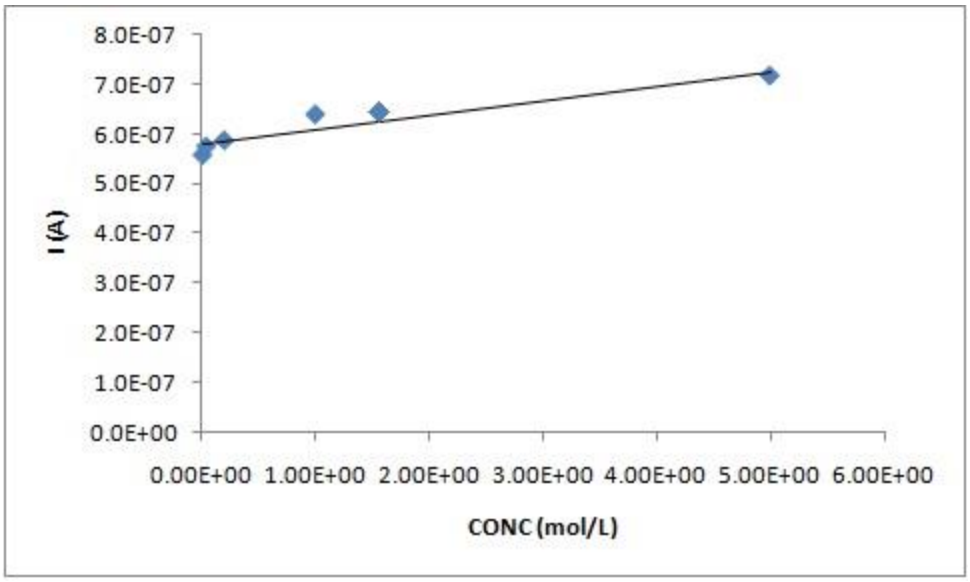

Figure 7.1. Calibration graph obtained for p53 using the modified graphene paste based sensor.

7.3.2 Selectivity of the Electrochemical Sensor

Mixed solution method was used as described above for the assessment of the selectivity of the proposed electrochemical sensor. The values obtained for the amperometric selectivity coefficients are shown in Table 7.1.

Table 7.1 Selectivity coefficients obtained for the electrochemical sensor.

Interferent	Amperometric selectivity coefficient
L-aspartic acid	4.00×10^{-3}
D-aspartic acid	4.07×10^{-4}
L-glutamine	4.17×10^{-4}
D-glutamine	4.68×10^{-4}
CEA	1.99×10^{-6}

The amperometric selectivity coefficients were determined using the following equation:

$$K\tilde{\imath}, j(amp) = \left(\frac{\Delta It}{\Delta Ii} - 1\right) * \frac{ci}{cj}$$

where $K_{i,\,j\,(amp)}$ is the amperometric selectivity coefficient, $\Delta I_t = \Delta I_t - \Delta I_b$, where ΔI_t is the total intensity of the current, ΔI_b is the intensity of the current recorded for blank solution, $\Delta I_i = \Delta I_i - \Delta I_b$,

where ΔI_i is the intensity of the current registered for main ion, c_i and c_j are the concentrations of the main ion and the interfering ions.

The values obtained for the amperometric selectivity coefficients shown that L-aspartic acid is slightly interfering in the determination of p53, while D-aspartic acid, L-glutamine, D-glutamine and CEA did not interfere in the assay of p53.

7.4 Determination of p53 in Whole Blood Samples

Five whole blood samples were analyzed using the proposed electrochemical sensor. No pretreatment was done before the measurements. The DPV was used to analyze p53 in blood samples. The cell was filled with the whole blood and the peak height was measured. The results of the differential pulse voltammetry measurements are shown in Table 7.2.

An example of voltammogram obtained from the measurement using DPV mode for determination of p53 in whole blood sample is illustrated in Figure 7.2.

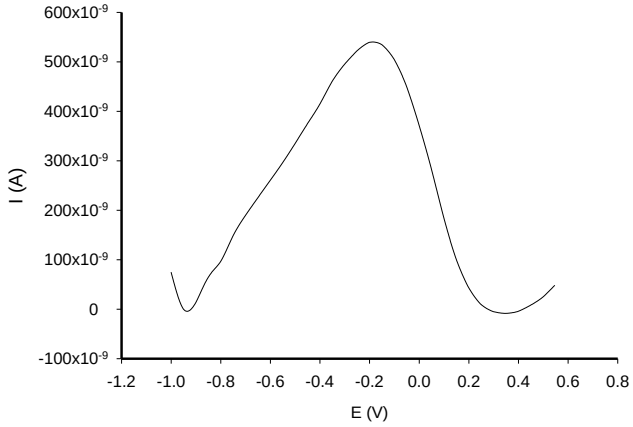

Figure 7.2. Example of voltammogram obtained for the assay of p53 in whole blood sample.

Table 7.2 Determination of p53 in whole blood samples using the electrochemical sensor and ELISA.

Sample No.	**ng mL^{-1}, p53**	
	ELISA	**Electrochemical sensor***
1	39.87	40.00±0.09
2	30.95	31.00±0.12

3	36.15	36.10±0.13
4	23.07	23.00±0.10
5	32.30	32.21±0.12

*N=10

The results shown a very good correlation between the results obtained using ELISA (a standard method used in the clinical laboratories) and the results obtained using the electrochemical sensors in DPV mode.

7.5 Conclusions

The proposed electrochemical sensor showed very good results for the recovery test which makes it a reliable tool for measuring p53 in whole blood samples. The sensor was highly sensitive, and exhibited excellent selectivity for the detection of p53 from blood samples.

The advantages of the proposed method versus techniques like ELISA are: it is a simple and easy method performed with low cost, short analysis time, and low limit of quantification, contributing to the diagnosis at a very early stage the gastric cancer.

Conclusions and Future Work

Different 2D and 3D stochastic sensors and microsensors were design, characterized and utilized for molecular recognition of amino acids (aspartic acid, arginine, glutamine), maspin, and p53.

Enantioanalysis of aspartic acid is essential for fast and early diagnosis of some diseases, like gastric cancer. Therefore, two 3D stochastic sensors based on graphene doped with Sulphur, and protoporphyrin IX were proposed as new tools for the screening test of whole blood. The high sensitivity, selectivity and enantioselectivity made them good candidates as new tools for the screening tests of whole blood for L- and D-aspartic acid. The proposed sensors had as features application in clinical analysis for fast recognition and quantification of the enantiomers of aspartic acid in order to have the correct and fast diagnosis related to these enantiomers, like gastric cancer.

Two 3D enantioselective needle stochastic sensors based on graphene decorated with N and S atoms were designed, characterized, validated and used for the enantioanalysis of arginine in biological samples (whole blood and gastric tumoral tissue samples) collected from patients confirmed with gastric cancer and from healthy volunteers. The results show that the presence of D-arginine can indicate at an early stage the presence of gastric cancer, and also can make the difference between the gastric cancer and gastric ulcer. The main feature of the proposed stochastic sensors is their utilization for the early diagnosis of gastric cancer.

A 2D enantioselective disposable stochastic sensor was proposed for the enantioanalysis of glutamine in whole blood and gastric tumor tissue samples. The high sensitivity of the sensor as well its wide working concentration range made possible the analysis of samples from confirmed patients with gastric cancer, but also from healthy volunteers. The main feature is its utilization for fast screening tests for the early detection of gastric cancer, based on the identification of D-glutamine, the quantification of L-, and D-glutamine, and determination of enantiomeric excess, especially that the sensors were connected to a mobile device able to record and read the diagrams.

Two stochastic microsensors based on graphene co-doped with N and S, and modified with α-cyclodextrin and maltodextrin, were designed, characterized, and validated for the pattern recognition and quantification of maspin in whole blood, gastric tumor tissue, saliva, and urine. The results obtained proved that the two stochastic microsensors are powerful tools for the fast-

screening tests of whole blood, tumor tissue, saliva, and urine for maspin in order to establish a fast diagnostic of gastric cancer.

Disposable stochastic sensors were designed using nanolayer deposition of a graphene nanocomposite material (nanographene - nanogold) on silk, plastic, and paper, for molecular recognition and quantification of maspin in biological samples. The main advantages of these sensors are: low cost, no sample preparation was needed, high sensitivity and reliability of the measurements, and no cross contamination, as they are just used once for the measurements.

The proposed electrochemical sensor showed very good results for the recovery test which makes it a reliable tool for measuring p53 in whole blood samples. The sensor was highly sensitive, and exhibited excellent selectivity for the detection of p53 from blood samples. The advantages of the proposed method versus techniques like ELISA are: it is a simple and easy method performed with low cost, short analysis time, and low limit of quantification, contributing to the diagnosis at a very early stage the gastric cancer.

Future work

The features of the proposed stochastic sensors, and of the screening method is their utilization in clinical laboratories for whole blood, urine, and saliva samples analysis, and in the laboratories of anatomopathology for tumor tissue analysis, as alternative for the semiquantitative colorimetric analysis, being a highly reliable and cost-effective type of tools and analysis. The method will help with the fast diagnosis of gastric cancer.

Therefore, a next step in their validation will be performed – mainly taking them to the clinics and hospitals where they can be used for screening tests.

Selected References

[1] Disse E., Bussier A. L., Veyrat-Durebex C., Deblon N., Pfluger P. T., Tschöp M. H., Laville M., Rohner-Jeanrenaud F., Peripheral ghrelin enhances sweet taste food consumption and preference, regardless of its caloric content, **Physiol. Behav.**, **vol.101**, no.2, 2010, 277-281.

[2] Fujiwara S., Imada T., Nakagita T., Okada S., Nammoku T., Abe K., Misaka T., Sweeteners interacting with the transmembrane domain of the human sweet-taste receptor induce sweet-taste synergism in binary mixtures, Food Chem., **vol.130,** no.3, 2012, 561-568.

[3] Gardner C., Wylie-Rosett J., Gidding S. S., Steffen L. M., Johnson R. K., Reader, D., Lichtenstein, A. H, Nonnutritive Sweeteners: current use and health perspectives, Diabetes Care, **vol.35**, no.8,2012, 1798-1808.

[4] Huth P. J., Fulgoni V. L., Keast D. R., Park K., Auestad N.,Major food sources of calories, added sugars, and saturated fat and their contribution to essential nutrient intakes in the U.S. diet: Data from the national health and nutrition examination survey (2003-2006), Nutr. J., **vol.12**, no. 1, article no. 116, 2013, 1-10.

[5] Ferlay J., Shin H.R., Bray F., Forman D., Mathers C., Parkin D.M. Estimates of worldwideburden of cancer in 2008: GLOBOCAN 2008. Int J Cancer, 2010,127,2893-2917.

[6] Leal MF, Assumpção PP, Smith MC, Burbano RR. Searching for Gastric Cancer BiomarkersThroughProteomicApproaches. J GastroenterolHepatol, 2014, 3(3),989-995.

[7] Braik T., Gupta S., Poola H., Jain P., Beiranvand A., Lad T.E., Hussein L. Carcino embryonic antigen (CEA) elevation as a predictor of better response to first line pemetrexed in advanced lung adenocarcinoma. J. Thorac. Oncol. 2012, 7, S310.

[8] Yu D.H., Li J.H., Wang Y.C., Xu J.G., Pan P.T., Wang, L. Serum anti-p53 antibody detection in carcinomas and the predictive values of serum p53 antibodies, carcino-embryonic antigen and carbohydrate antigen 12–5 in the neoadjuvant chemotherapy treatment for III stage non-small cell lung cancer patients. Clin. Chim. Acta 2011, 412, 930–935

[9] Shimada H., Noie T., Ohashi M., Oba K., Takahashi Y. Clinical significance of serum tumor markers for gastric cancer.

[10] Schwartzenberg-Bar-Yoseph F., Armoni M., Karnieli E., The tumor suppressor p53 down-regulates glucose transporters GLUT1 and GLUT4 gene expression, Cancer Res., 64(7), 2004, 2627-33.

[11] Zhang J., Xu Z.W., Yu L.X., Chen M.L., Li K., Assessment of the potential diagnostic value of serum p53 antibody for cancer: a meta-analysis. PLoS One, 9(6), 2014.

[12] Uchino S., Noguchi M., Ochiai A., Saito T., Kobayashi M., Hirohashi S., p53 mutation in gastric cancer: a genetic model for carcinogenesis is common to gastric and colorectal cancer, Int J. Cancer., 54(5), 1993, 759–764.

[13] Karim S., Correlation of p53 over-expression and alteration in p53 gene detected by polymerase chain reaction-single strand conformation polymorphism in adenocarcinoma of gastric cancer patients from India, World J. Gastroentero., 15(11), 2009, 1381–1387.

[14] Otani K., Li X.X., Arakawa T., Chan F.K.L., Yu J., Epigenetic-mediated tumor suppressorgenes as diagnostic or prognostic biomarkers in gastric cancer, Expert Rev. Mol. Diagn.,13(5), 2013, 445–455.

Annex 1

PAPERS PRESENTED AT CONFERENCES

ORAL PRESENTATIONS

1. Fast screening tests for early diagnosis of gastric cancer, based on molecular recognition and assay of maspin in biological samples, Mihaela Iuliana Bogea, Raluca-Ioana Stefan-van Staden, Ruxandra Maria Ilie-Mihai, Damaris-Cristina Gheorghe, 240th ECS Meeting, Orlando, FL, USA, October 10-14, 2021
2. Enantioanalysis – a step forward for early detection of gastric cancer, Mihaela Iuliana Bogea, R.I. Stefan-van Staden, R.M. Ilie-Mihai, D.C. Gheorghe, 7th International Conference on Sensors Engineering and Electronics Instrumentation Advances (SEIA' 2021), Palma de Mallorca, Mallorca (Balearic Islands), Spain, 22-24 September 2021.

Annex 2

PAPERS PUBLISHED IN ISI JOURNALS
(Total I.F.=17.631)

1. Enantioanalysis of aspartic acid using 3D stochastic sensors
   IM Bogea, RI Stefan-van Staden, DC Gheorghe, RM Ilie-Mihai
   Anal.Lett, 55(1), 85-92, 2022 (**I.F.=2.267**)

2. 2D Disposable Stochastic Sensors for Molecular Recognition and Quantification of Maspin in Biological Samples
   RI Stefan-van Staden, RM Ilie-Mihai, DC Gheorghe, IM Bogea, M Badulescu
   Microchimica Acta, 189, 101, 2022 (**I.F.=6.408**)

3. Stochastic microsensors based on modified graphene for pattern recognition of maspin in biological samples
   RI Stefan-van Staden, IM Bogea, RM Ilie-Mihai, DC Gheorghe, M Coros, SM Pruneanu
   Anal Bioanal Chem, 414(12), 3667-3673, 2022 (**I.F.=4.478**)

4. NS Decorated Graphenes Modified with 2,3,7,8,12,13,17,18-Octaethyl-21H,23H-Porphine Manganese (III) Chloride Based 3D Needle Stochastic Sensors for Enantioanalysis of Arginine - a Key Factor in the Metabolomics and Early Detection of Gastric Cancer
   RI Stefan-van Staden, MI Bogea, RM Ilie-Mihai, DC Gheorghe, HY Aboul-Enein, M Coros, SM Pruneanu
   Anal. Bioanal.Chem., 414(22), 6521–6530, 2022 (**I.F.=4.478**)

5. Determination of p53 from whole blood samples using an electrochemical sensor based on graphene decorated with N and S
   IM Bogea, RM Ilie-Mihai, RI Stefan-van Staden
   Sci Bull UPB, 84(3), 121-130, 2022